

Mass Spectrometry in Process Development of Therapeutic Proteins

Pavel V Bondarenko
Amgen Process Development
CASSS MASS SPEC 2019
September 20, 2019

AMGEN[®]

Pioneering science delivers vital medicines™

Mass spectrometry at different steps of Process Development

Molecule assessment

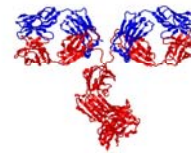
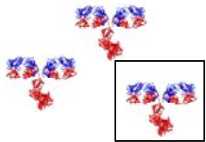
Clone selection and cell aging stability

Bioprocess and media optimization

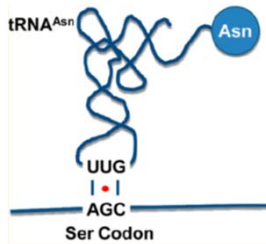
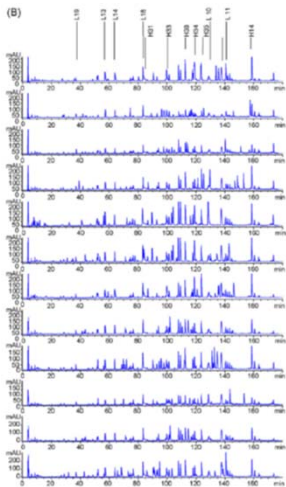
Elucidation of structure and function

QC

PK and biotransformations

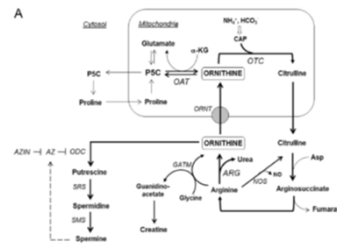


MAM

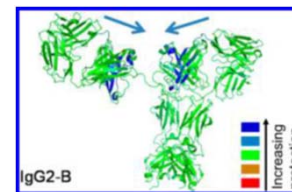
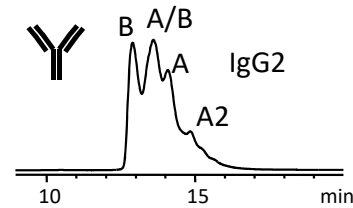


Sequence variants analysis (mutations, misincorporations, deletions, undesired enzymatic modifications)

Select most chemically stable variant/construct

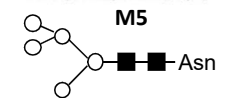
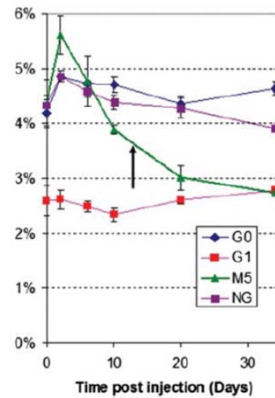


Systems biology (proteomics, metabolomics) of industrial mammalian cells for higher productivity and control of product quality (glycosylation)



(Zhang A et al., 2015)

Assessment of criticality of chemical modifications (attributes) by correlating structure and function (potency, binding, PK)



Assessment of criticality by correlating modifications to PK





- **Methods:**

- Intact, reduced RP LC-MS, peptide mapping
- IEX-MS, SEC-MS
- Sample preparation

- **Molecule (manufacturability) assessment**

- **Clone selection and cell aging stability.** Sequence variants analysis for mutations, misincorporations, undesired enzymatic modifications.

- **Bioprocess and media optimization.** Systems biology to increase productivity and control product quality (glycosylation). Host cell protein assessment.

- **Elucidation of structure and function, stability.**

- Example: IgG2 disulfide connectivity

- **PK and biotransformations in blood**

- Example: impact of high mannose 5 (M5) glycosylation

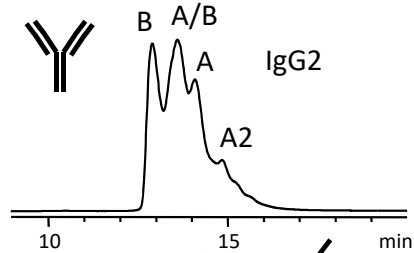


RP LC-UV-MS analysis of intact, reduced protein and peptide mapping

Methods

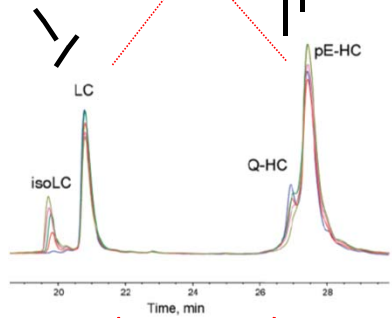
RP LC-UV-MS of intact and subunit

HPLC:
Zorbax SB C8 at 75°C,
1 or 2-Propanol,
0.1% TFA
Dillon et al, 2008



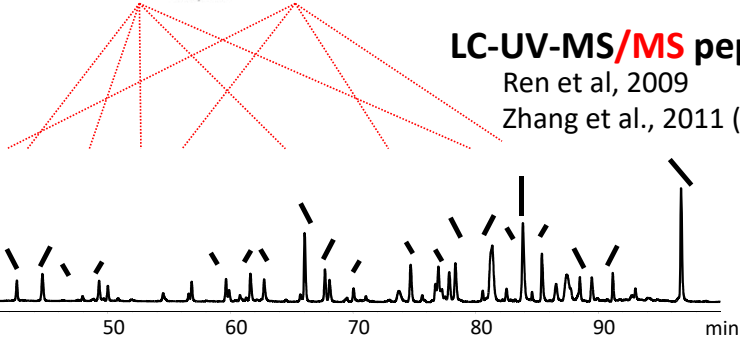
RP LC-UV-MS of reduced

Dillon et al, 2006
Rehder et al, 2008



LC-UV-MS/MS peptide map:

Ren et al, 2009
Zhang et al., 2011 (MassAnalyzer)



Modifications / attributes

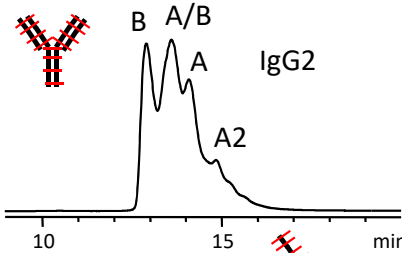
- Disulfide connectivity including free thiol (-Cys-H), open disulfides (-Cys-H H-Cys-), monosulfide (-Cys-S-Cys-), trisulfide (-Cys-S-S-S-Cys-), half-molecules, IgG2 disulfide heterogeneity, disulfide scrambling, glycosylation pairing, glycation.
- Unstable modifications: N-terminal glutamine, succinimide intermediate, deamidation.
- Products of DNA/RNA deletion.
- Fragmentation.
- Several other modifications: iso-Asp, oxidation, N-terminal Q to pyroE.
- Products of DNA/RNA deletion.
- A wide array of chemical modifications, sequence variants **and their locations**.

LC-UV-MS of intact/subunit and reduced protein and peptide mapping can reliably cover practically all chemical modifications

RP LC-UV-MS/MS analysis of intact, reduced protein (with top-down fragmentation)

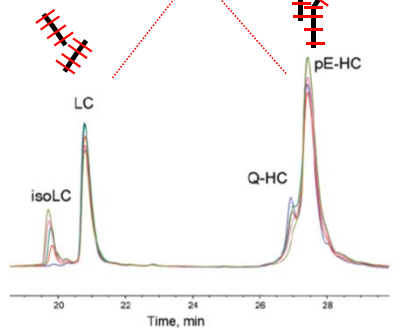
Methods

RP LC-UV-MS of intact and subunit



HPLC:
Zorbax SB C8 at 75°C,
1 or 2-Propanol,
0.1% TFA
Dillon et al, 2008

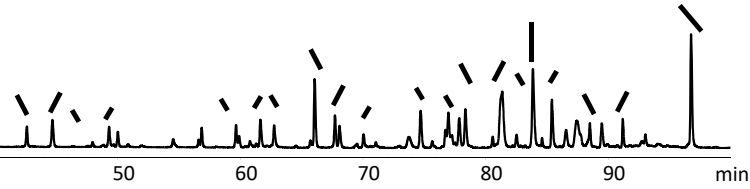
RP LC-UV-MS of reduced



Dillon et al, 2006
Rehder et al, 2008

LC-UV-MS/MS peptide map:

Ren et al, 2009
Zhang et al., 2011 (Mass Analyzer)



Modifications / attributes

- Disulfide connectivity including free thiol (-Cys-H), open disulfides (-Cys-H H-Cys-), monosulfide (-Cys-S-Cys-), trisulfide (-Cys-S-S-S-Cys-), half-molecules, IgG2 disulfide heterogeneity, disulfide scrambling, glycosylation pairing, glycation and their locations.
- Unstable modifications: N-terminal glutamine, succinimide intermediate, deamidation.
- Products of DNA/RNA deletion.
- Fragmentation.
- Several other modifications: iso-Asp, oxidation, N-terminal Q to pyroE and their locations.
- Products of DNA/RNA deletion.
- A wide array of chemical modifications, sequence variants and their locations.

- LC-UV-MS of intact/subunit and reduced protein with top-down fragmentation has been applied for characterization of a number of modifications.
- In the future, the intact and reduced protein analysis has a potential to replace peptide mapping, but sensitivity needs to be improved further.

Example: RP LC-UV-MS of intact IgG2 for detection of succinimide accumulated in a pH 5 formulation

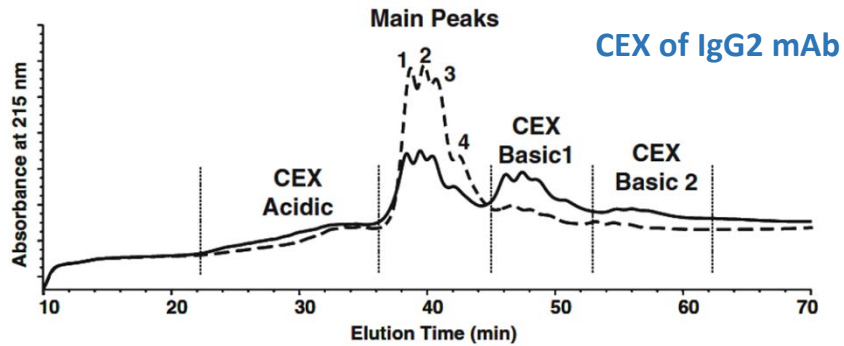
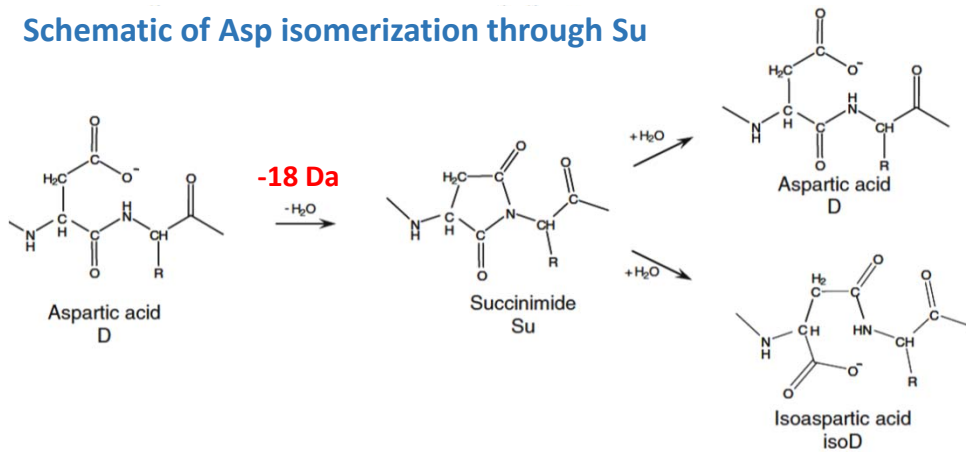
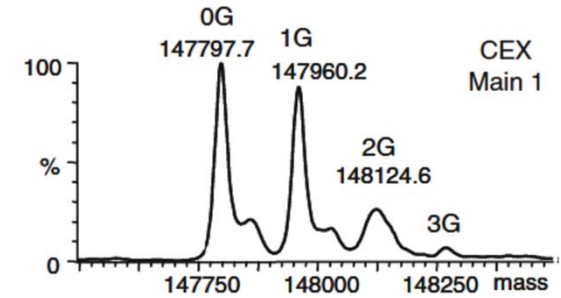


Fig. 1. CEX chromatograms of the monoclonal human IgG2 antibody stored at -70°C (broken line) and after 2 weeks at 45°C (solid line) in a pH 5 buffer.

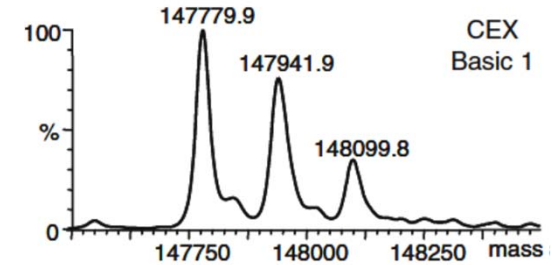
Schematic of Asp isomerization through Su



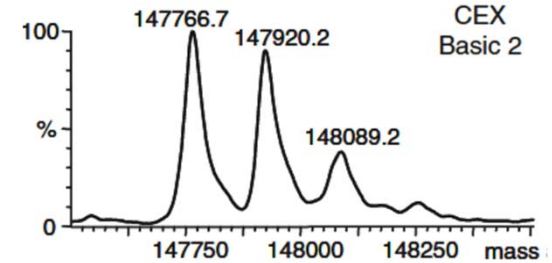
Deconvoluted mass spectra of CEX peaks



(-18 Da) 1 succinimide



(-31 Da) 2 x succinimide

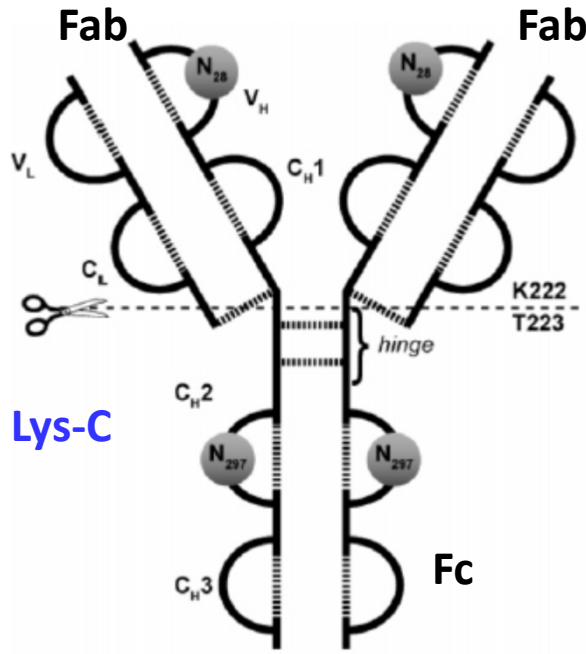


- After an accelerated stress, IgG2 generated two basic peaks with an unknown modification, later identified as succinimide of Asp30
- Tryptic peptide mapping with overnight digestion could not reveal the root cause, because it hydrolyzed succinimide to Asp and iso-Asp
- Intact LC-MS-MS analysis of collected CEX fractions revealed unstable succinimide intermediate with -18 Da mass change.

Chu et al., 2007

Xiao et al., 2007

RP LC-UV-MS of IgG1 subunits Fab and Fc after limited proteolysis with Lys-C endoproteinase



The antibody (2 mg/ml) was incubated in the presence of endoproteinase Lys-C using an enzyme/substrate weight ratio of 1:400 in 100 mM Tris-HCl buffer at pH 8.0 and 37 °C for 20 min.

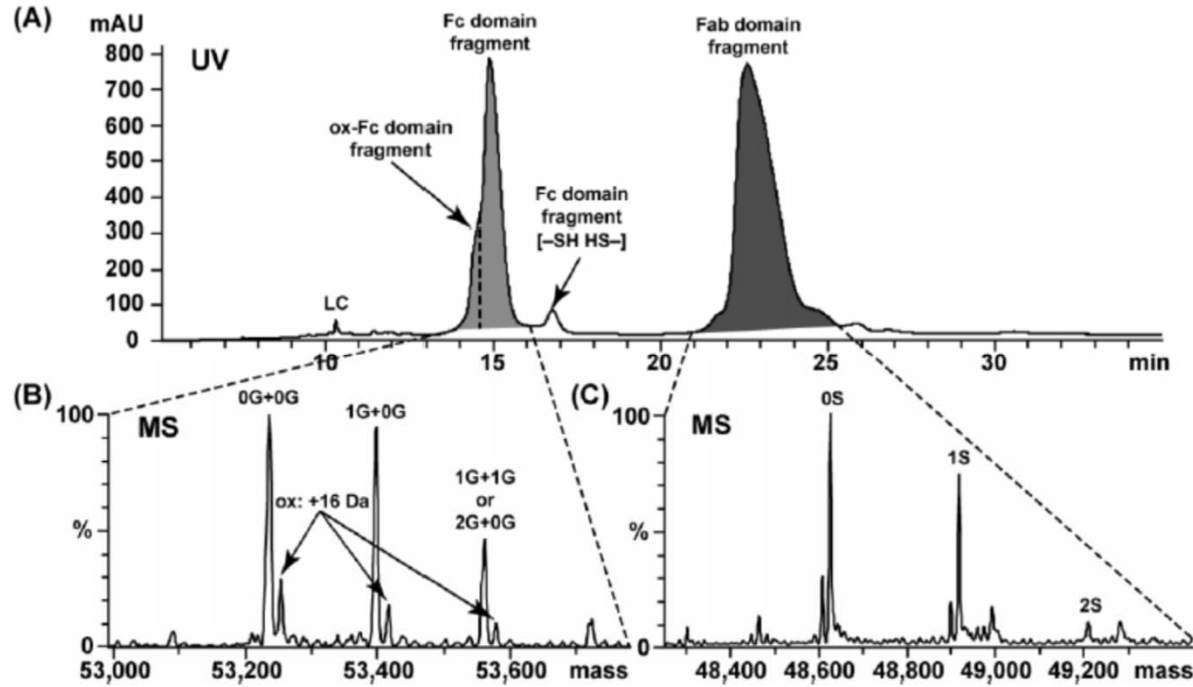


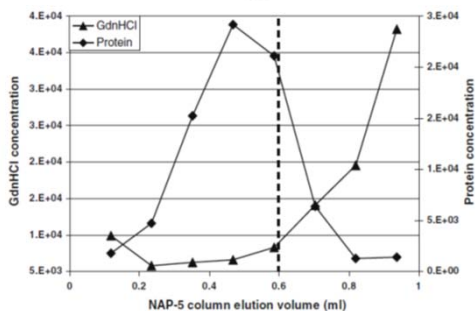
Figure 7. Characterization of the carbohydrate heterogeneity of the IgG1 antibody containing two glycosylation sites by limited Lys-C proteolysis

Kleemann et al., 2008

- Limited proteolysis of IgG1 with Lys-C endoproteinase produces Fab and Fc subunits after cleavage above the hinge (DK/THTCPPC)

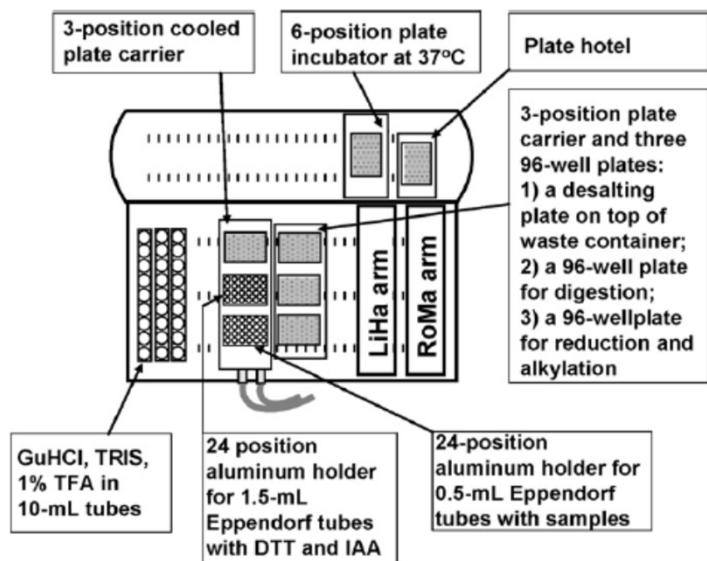
Development of rapid and automated protein digestion

Rapid tryptic digestion



Manual 30-minute digestion.
 Better removal of guanidine before tryptic digestion
 Ren et al., 2009

Automated tryptic digestion using buffer exchange in TECAN autosampler



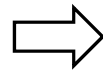
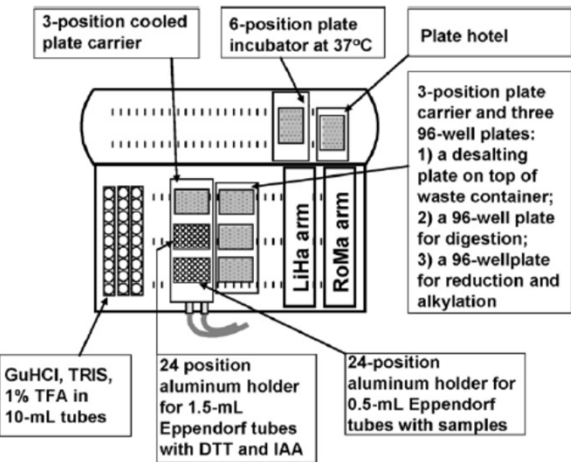
27 mAbs and 4 Fc-fusion proteins were automatically digested during 5-hour digestion with second trypsin addition after 2 hours
 Chelius et al., 2008

Automated Lys-C, Glu-C digestion using dilutions in a common HPLC autosampler

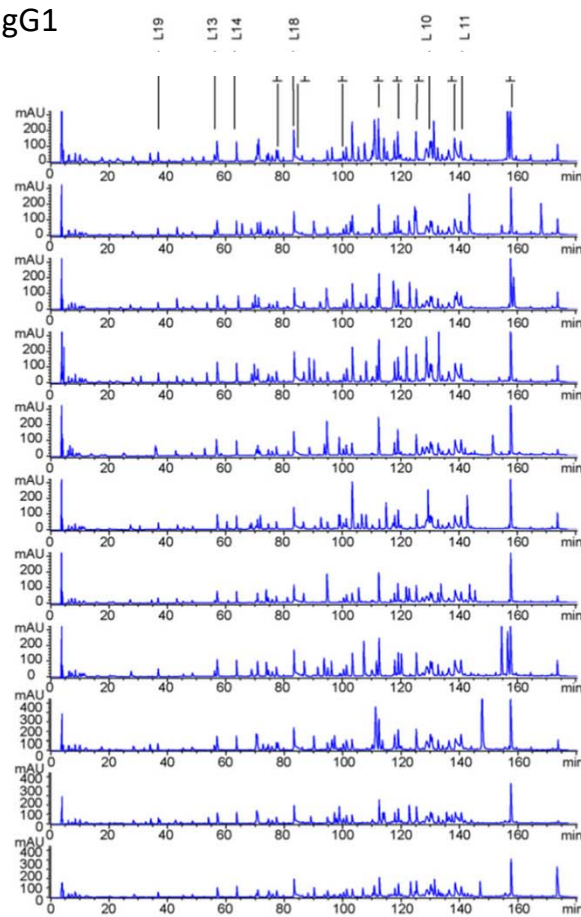


The method is optimal for higher protein concentrations above 10 mg/ml
 Richardson et al., 2011

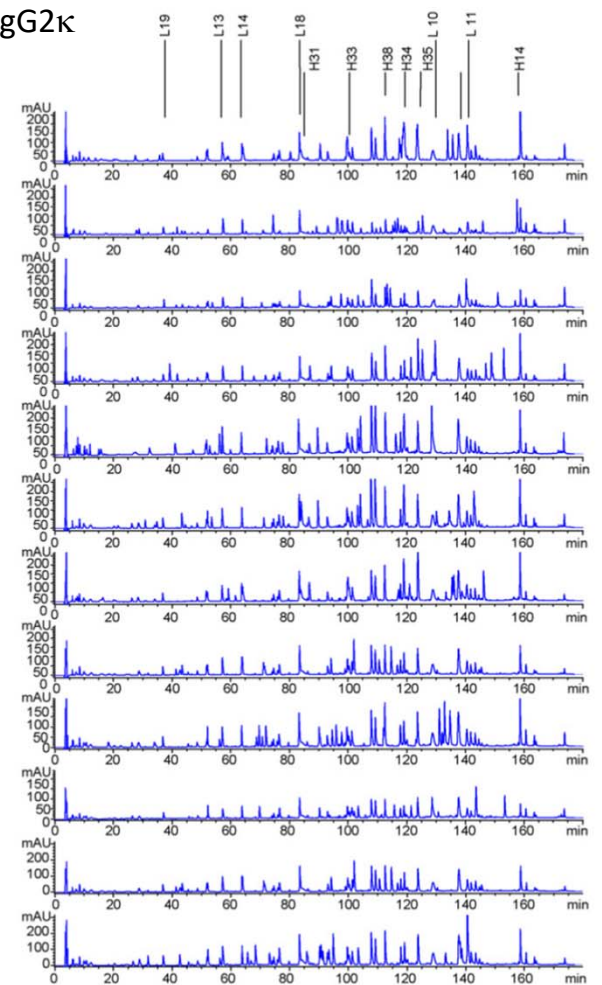
Automated tryptic digestion using buffer exchange in TECAN autosampler



IgG1



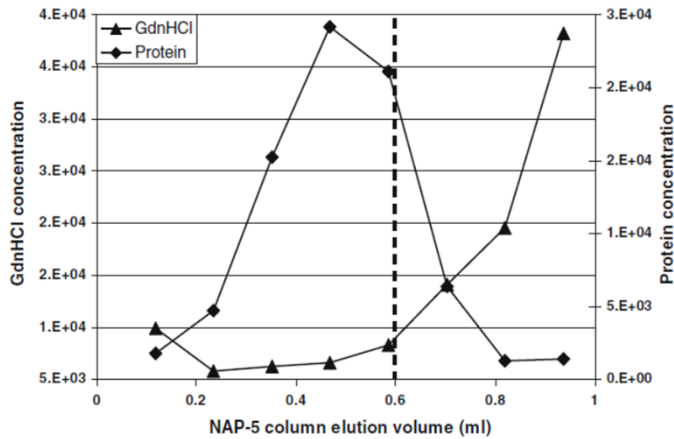
IgG2κ



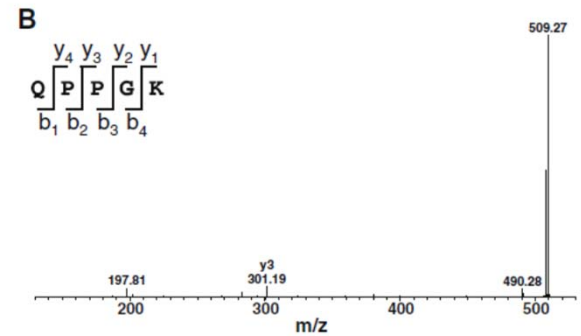
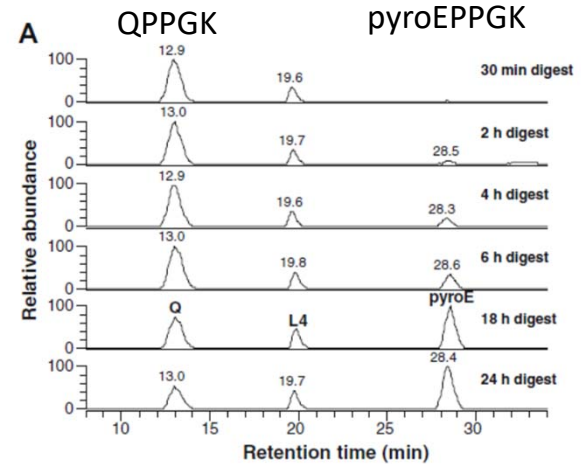
Chelius et al., 2008

- Buffer exchange by size exclusion NAP-5 cartridge.
- 27 mAbs and 4 Fc-fusion proteins were automatically digested by 5-hour tryptic digestion with second trypsin addition after 2 hours.
- The systems had been used for formulation development, molecule assessment

Rapid 30-minute tryptic digestion

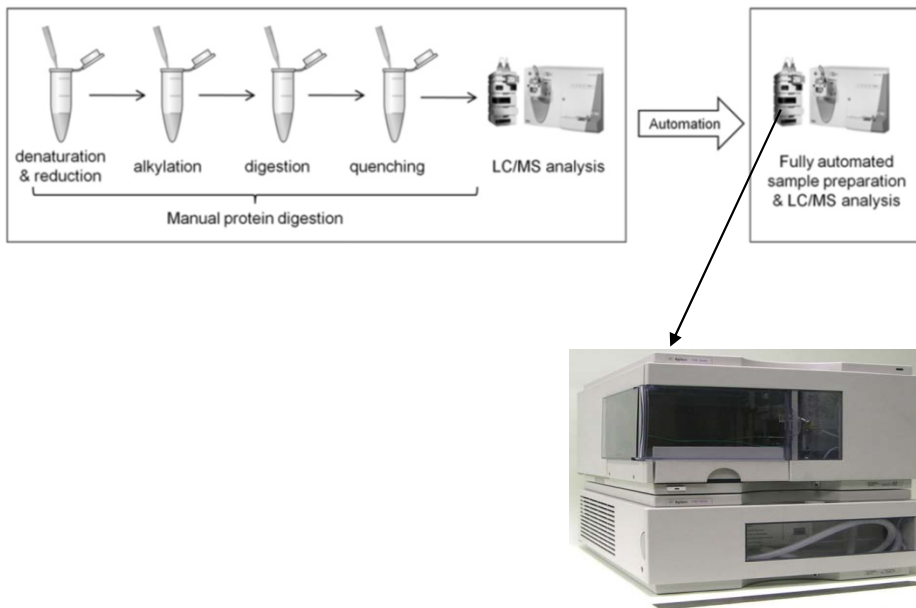


Ren, D et al., 2009

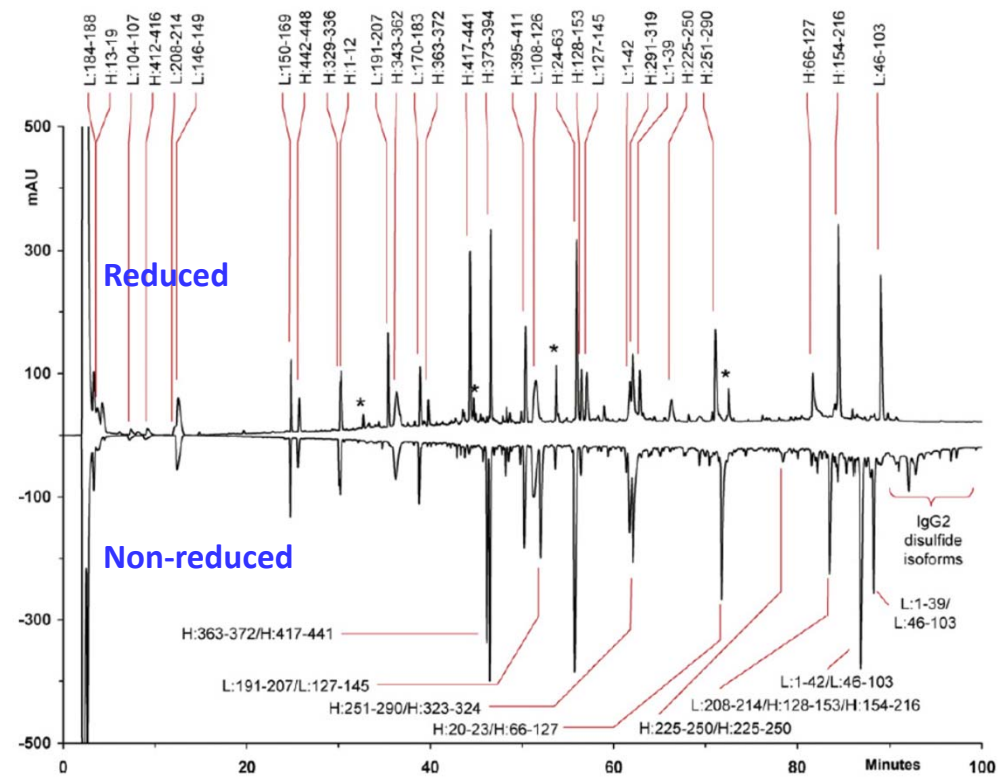


- More complete removal of guanidine by size-exclusion NAP-5 column before tryptic digestion is important for rapid digestion
 - Protocol-induced deamidation, N-terminal Q cyclization to pyroE, hydrolysis of succinimide and trypsin self-digestion were minimized

Automated digestion using a commonly available HPLC autosampler



Lys-C peptide map of IgG2



Richardson et al., 2011

- The method is optimal for higher protein concentrations above 10 mg/ml
- Lys-C, Glu-C non-reduced and reduced digestions were implemented on the system



Sequence variant analysis - misincorporations

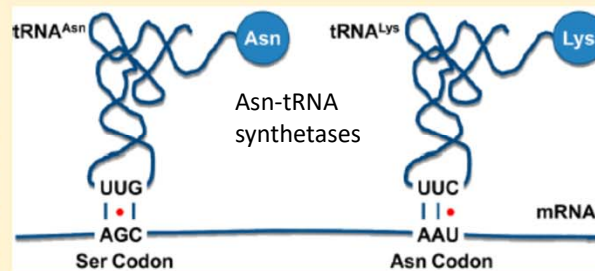
G/U and Certain Wobble Position Mismatches as Possible Main Causes of Amino Acid Misincorporations

Zhongqi Zhang,* Bhavana Shah, and Pavel V. Bondarenko

Process and Product Development, Amgen Inc., Thousand Oaks, California 91320, United States

Supporting Information

ABSTRACT: A mass spectrometry-based method was developed to measure amino acid substitutions directly in proteins down to a level of 0.001%. When applied to recombinant proteins expressed in *Escherichia coli*, monoclonal antibodies expressed in mammalian cells, and human serum albumin purified from three human subjects, the method revealed a large number of amino acid misincorporations at levels of 0.001–0.1%. The detected misincorporations were not random but involved a single-base difference between the codons of the corresponding amino acids. The most frequent base differences included a change from G to A, corresponding to a **G(mRNA)/U(tRNA)** base pair mismatch during translation. We concluded that under balanced nutrients, **G(mRNA)/U(tRNA)** mismatches at any of the three codon positions and certain additional wobble position mismatches (**C/U and/or U/U**) are the main causes of amino acid misincorporations. The hypothesis was tested experimentally by monitoring the levels of misincorporation at several amino acid sites encoded by different codons, when a protein with the same amino acid sequence was expressed in *E. coli* using 13 different DNA sequences. The observed levels of misincorporation were different for different codons and agreed with the predicted levels. Other less frequent misincorporations may occur due to **G(DNA)/U(mRNA)** mismatch during transcription, mRNA editing, **U(mRNA)/G(tRNA)** mismatch during translation, and tRNA mischarging.



The universal genetic code and **Ser codon with frequent misincorporation**

		Second letter					
		U	C	A	G		
First letter	U	UUU } Phe UUC } UUA } Leu UUG }	UCU } Ser UCC } UCA } UCG }	UAU } Tyr UAC } UAA Stop UAG Stop	UGU } Cys UGC } UGA Stop UGG Trp	U	C
	C	CUU } Leu CUC } CUA } CUG }	CCU } Pro CCC } CCA } CCG }	CAU } His CAC } CAA } Gln CAG }	CGU } Arg CGC } CGA } CGG }	U	C
	A	AUU } Ile AUC } AUA } AUG Met	ACU } Thr ACC } ACA } ACG }	AAU } Asn AAC } AAA } AAG } Lys	AGU } Ser AGC } AGA } AGG } Arg	U	C
	G	GUU } Val GUC } GUA } GUG }	GCU } Ala GCC } GCA } GCG }	GAU } Asp GAC } GAA } Glu GAG }	GGU } Gly GGC } GGA } GGG }	U	C
						A	G

(Zhang et al., 2013)

- Several rules were uncovered for misincorporations, typically at ~0.001% - 0.1%, which facilitated their automated identification.
- Under balanced nutrients, G(mRNA)/U(tRNA) mismatches at any of the three codon positions and certain additional wobble position mismatches (C/U and/or U/U) are the main causes of amino acid misincorporations.
- G/U mismatches are known to occur frequently in nucleic acid secondary structures and mRNA/tRNA interactions due to their similar binding energies as conventional Watson-Crick base pairs.

Sequence variant analysis - misincorporations

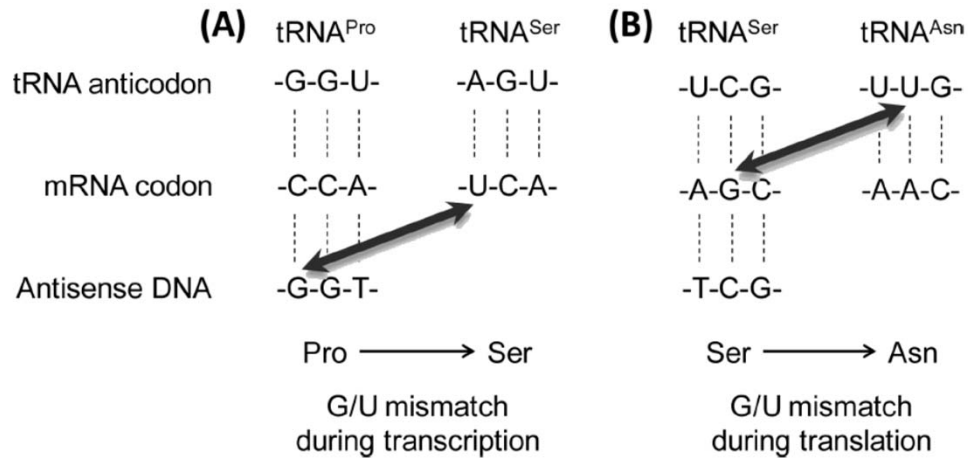


Figure 1. (A) Amino acid misincorporations involving a C → U base change in their mRNA codons can be explained by a G^{DNA}/U^{mRNA} base pair mismatch (indicted by the double arrow) during transcription. (B) Amino acid misincorporations involving a G → A base change can be explained by a G^{mRNA}/U^{tRNA} base pair mismatch during translation.

- Several rules were uncovered for misincorporations which facilitated their automatic identification by MassAnalyzer software algorithm
- They are typically at low level of 0.01% - 0.1%

(Zhang et al., 2013)

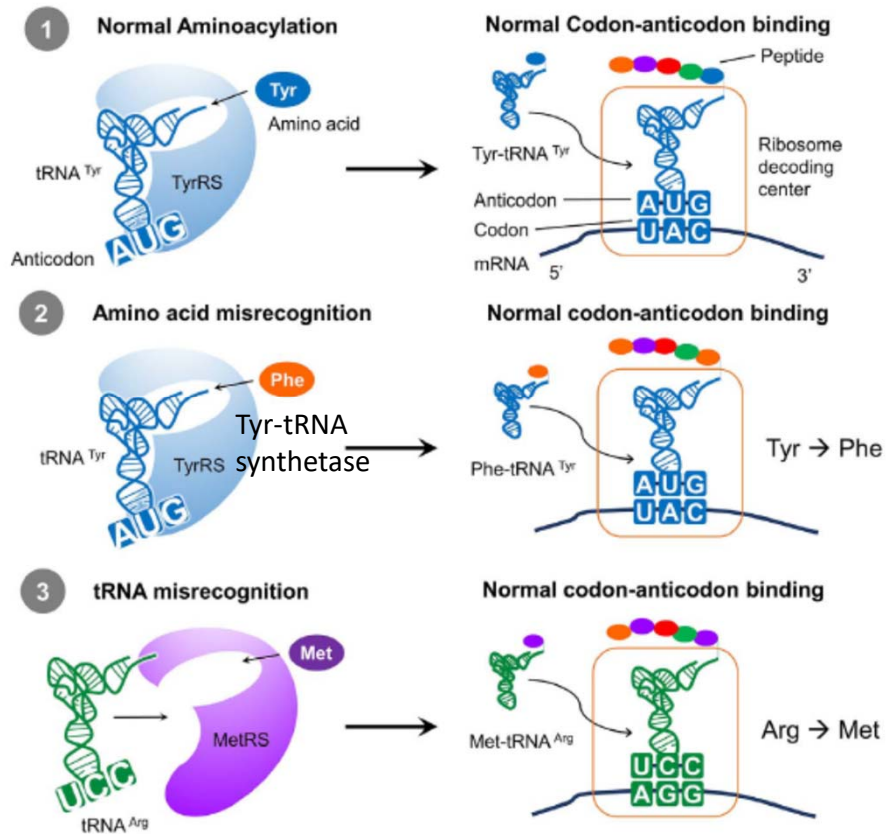
Table 6. Predicted Most Possible Amino Acid Misincorporations by a G^{mRNA}/U^{tRNA} Mismatch or a Third-Base C/U or U/U Mismatch during Codon Recognition^a

amino acid	codons	predicted misincorporated amino acids	
		G/U mismatch	third-base mismatch
A	GCU, GCC, GCA, GCG	T	none
C	UGU, UGC	Y	W, stop
D	GAU, GAC	N	E
E	GAA, GAG	K	none
F	UUU, UUC	none	L
G	GGA, GGG	E, R	none
G	GGU, GGC	D, S	none
H	CAU, CAC	none	Q
I	AUU, AUC	none	M
I	AUA	none	none
K	AAA, AAG	none	none
L	all six codons	none	none
M	AUG	I	I
N	AAU, AAC	none	K
P	CCU, CCC, CCA, CCG	none	none
Q	CAA, CAG	none	none
R	CGA, CGG	Q	none
R	CGU, CGC	H	none
R	AGA, AGG	K	none
S	AGU, AGC	N	R
S	UCU, UCC, UCA, UCG	none	none
T	ACU, ACC, ACA, ACG	none	none
V	GUU, GUC, GUA	I	none
V	GUG	M	none
W	UGG	stop	stop
Y	UAU, UAC	none	stop
Stop	UAA, UAG, UGA	none	none

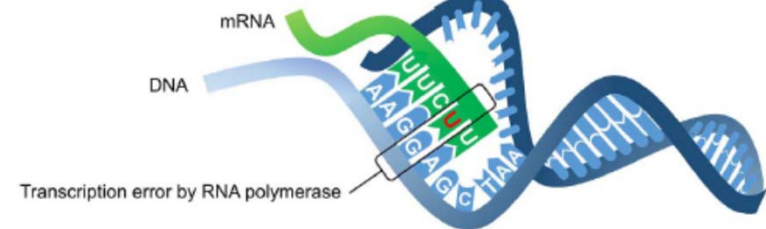
^aAmino acids with codon-dependent predictions are shown in bold.

Amino acid misincorporation mechanisms

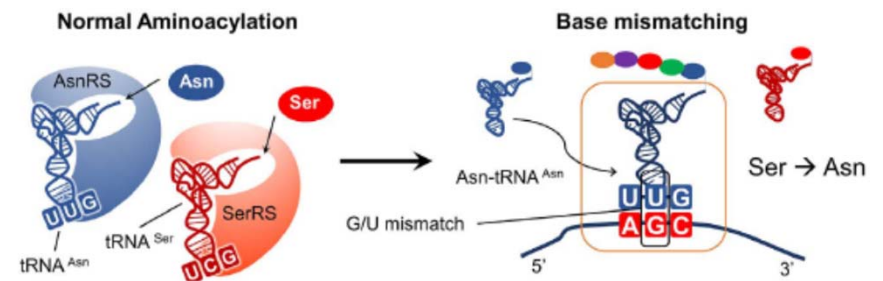
B Misacylation



A Transcription error



C Codon-anticodon mispairing



- Several mechanisms and rules were uncovered for misincorporations, which facilitated their automatic identification by MassAnalyzer software algorithm

Wong et al, 2018

Several common chemical modifications can be misidentified as mutations and misincorporations

Table S1. Common modifications that can be misidentified as amino acid substitutions.

Δ mass	Modification	Modification site ^c	Amino-acid substitutions ^d	Substitution Δ mass
-58.005	incomplete carboxymethylation ^a	Cm-C	D→G, E→A	-58.005
-57.021	incomplete carbamidomethylation ^a	Cam-C	N→G, Q→A	-57.021
-48.003	side chain (CH ₂ S) loss from Met ^e	M	Y→D	-48.036
-48.003	side chain (CH ₂ S) loss from Met ^e	M	F→V	-48.000
-44.026	gas-phase C ₂ H ₄ O loss ^f	T	T→G	-44.026
-44.026	gas-phase C ₂ H ₄ O loss ^f	T	M→S	-44.008
-43.990	CO ₂ loss	C-term, E, D	T→G, D→A	-43.990
-30.011	gas-phase formaldehyde loss ^g	C-term, ST	S→G, T→A	-30.011
-28.031	C ₂ H ₄ loss	P	R→K	-28.006
-23.016	His oxidation to Asn	H	H→N	-23.016
-18.011	H ₂ O loss ^h	DEST	F→E	-18.026
-17.027	NH ₃ loss	QNKR, Cam-C	N→P	-16.990
-14.02	unknown ⁱ	Cam-C	E→D, A→G, T→S, L→V, I→V, Q→N	-14.016
-14.016	CH ₂ loss ^e	M, P	E→D, A→G, T→S, L→V, I→V, Q→N	-14.016
-10.021	triple oxidation of Cys	Cm-C	P→S	-10.021
-0.984	amide formation ^h	C-term, Cm-C	D→N, E→Q	-0.984
0.984	deamidation ^h	NQ, Cam-C	I→N, L→N	0.959
3.995	oxidation of Trp to kynurenine ^h	W	P→T	3.995
13.975	oxidation products ^h	YW	T→D	13.979
13.975	oxidation products ^h	YW	D→E, G→A	14.016
15.01	unknown	YW	V→N	14.975
15.995	oxidation ^h	Virtually all	L→Q, I→Q	14.975
15.995	oxidation ^h	Virtually all	V→D	15.959
15.995	oxidation ^h	Virtually all	A→S, F→Y	15.995
21.982	Na adduct ^h	nonspecific	D→H	22.032
27.995	formylation	N-term, ST	K→R	28.006
31.990	double oxidation ^h	MWCY	P→Q	31.006
31.990	double oxidation ^h	MWCY	V→M	31.972
31.990	double oxidation ^h	MWCY	P→E	31.990
43.006	carbamylation	N-term, K	L→R, I→R	43.017
47.990	triple oxidation ^h	WC	V→F	48.000
57.021	carbamidomethylation ^a	CHK, Cam-C, N-term	G→N, A→Q	57.021
58.006	carboxymethylation ^a	CHK, Cm-C, N-term	K→W	57.984
58.006	carboxymethylation ^a	CHK, Cm-C, N-term	G→D, A→E	58.006
115.027	Asp residue ^b	N-term, C-term	X→D	115.027
128.095	Lys residue ^b	N-term, C-term	X→K	128.095
129.043	Glu residue ^b	N-term, C-term	X→E	129.043
156.101	Arg residue ^b	N-term, C-term	X→R	156.101

^aThese modifications are incorporated in MassAnalyzer to search before searching for amino-acid substitutions.

^bAsp, Lys, Glu and Arg residues are added to the N- or C-terminus through protease-catalyzed transpeptidation by Asp-N (Asp), Lys-C (Lys), Glu-C (Glu) or trypsin (Lys and Arg).

^cCm-C: carboxymethylated cysteine; Cam-C: carbamidomethylated cysteine.

^dX→Y represents that the X residue is replaced by a Y residue.

Table 4

Frequently observed false positives and their causes in LC-MS/MS-based sequence variant analysis, assuming peptide mass changes can be determined to within ± 0.03 Da.

False positive (one-base change)	False positive Δ mass	Cause/modification	True modification site ^a	Modification Δ mass
A → D	43.990	Double Na adduct	Nonspecific	43.964
A → E	58.005	Carboxymethylation	C, H, M, K, Cm-C, N-term	58.005
A → G	- 14.016	CH ₂ loss	M, P, Cam-C	- 14.016
A → S	15.995	Oxidation	Many	15.995
D → A	- 43.990	Gas-phase CO ₂ loss	C-term, E, D	- 43.990
D → G	- 58.005	Incomplete carboxymethylation	Cm-C	- 58.005
D → N	- 0.984	Amide formation	C-term, Cm-C	- 0.984
E → A	- 58.005	Incomplete carboxymethylation	Cm-C	- 58.005
E → D	- 14.016	CH ₂ loss	M, P, Cam-C	- 14.016
E → Q	- 0.984	Amide formation	C-term, Cm-C	- 0.984
F → V	- 48.000	CH ₂ S loss from Met	M	- 48.003
F → Y	15.995	Oxidation	Many	15.995
G → D	58.005	Carboxymethylation	C, H, M, K, Cm-C, N-term	58.005
H → N	- 23.016	Oxidation of His to Asn	H	- 23.016
I → N	0.959	Deamidation	N, Q, Cam-C	0.984
I → R	43.017	Carbamylation	N-term, K	43.006
I → V	- 14.016	CH ₂ loss	M, P, Cam-C	- 14.016
K → R	28.006	Formylation	N-term, S, T	27.995
L → R	43.017	Carbamylation	N-term, K	43.006
L → V	- 14.016	CH ₂ loss	M, P, Cam-C	- 14.016
M → T	- 29.993	Gas-phase H ₂ CO loss	C-term, S, T	- 30.011
N → D	0.984	Deamidation	N, Q, Cam-C	0.984
N → I	- 0.959	Amide formation	C-term, Cm-C	- 0.984
P → A	- 26.016	Double oxidation of Cys	Cm-C	- 26.016
P → S	- 10.021	Triple oxidation of Cys	Cm-C	- 10.021

- Several common modifications can be misidentified as amino acid substitutions (mutations, misincorporations)

- Sequence variant analysis still includes laborious manual verification and remains probably the most challenging analysis of therapeutic proteins

Zhang et al., 2013

Wong et al., 2018

Sequence variant analysis in Biopharmaceutical industry

MABS
2019, VOL. 11, NO. 1, 1–12
<https://doi.org/10.1080/19420862.2018.1531965>



PERSPECTIVE

OPEN ACCESS

Evolution of a comprehensive, orthogonal approach to sequence variant analysis for biotherapeutics

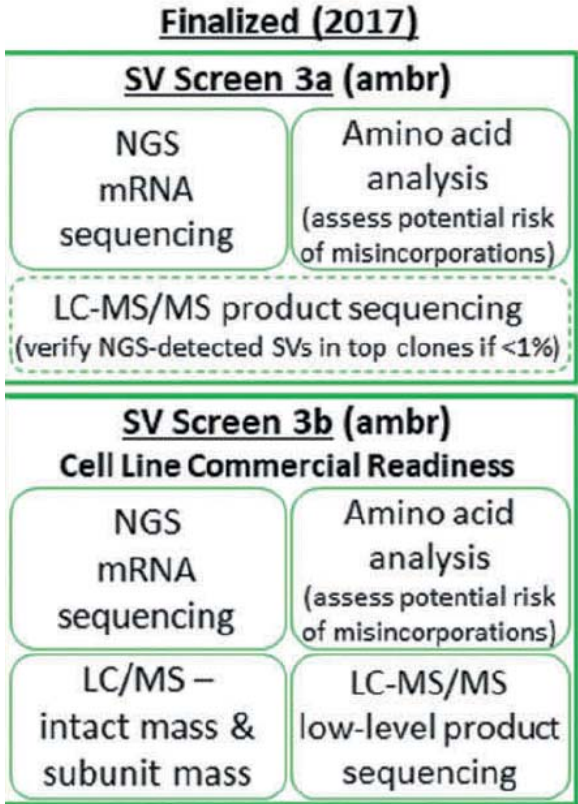
T. Jennifer Lin ^a, Kathryn M. Beal ^a, Paul W. Brown ^b, Heather S. DeGruttola ^a, Mellisa Ly ^a, Wenge Wang ^a, Chia H. Chu ^b, Robert L. Dufield ^b, Gerald F. Casperson ^b, James A. Carroll ^b, Olga V. Friese ^b, Bruno Figueroa Jr. ^a, Lisa A. Marzilli ^a, Karin Anderson ^a, and Jason C. Rouse ^a

^aBiotherapeutics Pharmaceutical Sciences, Pfizer, Inc, Andover, MA, USA; ^bBiotherapeutics Pharmaceutical Sciences, Pfizer, Inc, Chesterfield, MO, USA

Lastly, LC/MS-subunit analysis was maintained to ensure 100% sequence coverage for SV analysis, and to deliver the heightened characterization product quality assessments. And as discussed above, LC/MS-intact mAb analysis was added to orthogonally monitor the overall product proteoform quality profile, including N-glycosylation patterns, aglycosylation, terminal heterogeneity, trisulfides, and glycation. Thus, in Scheme 1, the two SV analysis checkpoints,

- The published SVA strategy describes an arsenal of methods including
- NGS mRNA sequencing
- LC/MS intact mass and subunit mass
- Amino acid analysis of media to assess potential risk of misincorporations
- LC-MS/MS low-level product sequencing

Lin et al., 2019



Sequence variant analysis – Biopharmaceutical industry survey

Biopharmaceutical Industry Practices for Sequence Variant Analyses of Recombinant Protein Therapeutics

John Valliere-Douglass, Lisa Marzilli, Aparna Deora, et al.

PDA Journal of Pharmaceutical Science and Technology 2019,
Access the most recent version at doi:[10.5731/pdajpst.2019.010009](https://doi.org/10.5731/pdajpst.2019.010009)

- The ability to confidently detect low level SVs has prompted 6 of the 11 companies polled to develop a specific, “optimized” LC-MS/MS peptide mapping methods for SVA.
- This optimization may include the use of multiple enzymes to maximize sequence coverage, selection of multiple charge states for quantitation, ... to reach better sensitivity and selectivity for SV detection.
- However, these “optimized” methods do not typically use a system suitability standard.
- In the survey, the number of samples analyzed for SVs by MS methods ranged broadly from <2 samples to >8 samples per project.
- LC/MS analysis of intact antibodies and subunits, as well as charge-based electrophoretic or chromatographic methods, have triggered a LC-MS/MS peptide mapping workflow to identify, localize, and quantify SVs.
- 6 of 11 respondents currently use NGS for SVA and are implementing this technology in clinical development to identify SVs in the genome and transcriptome of recombinant protein producing host cell lines.
- 0.5% was a more realistic threshold for NGS sensitivity in an industry setting.
- While several companies reported discarding a cell line with >1% SV, this was in reference to new product cell lines under development and not commercial programs.
- Labs typically require 3-8 weeks to complete data analysis

Valliere-Douglass *et al.*, 2019



Metabolomics analysis of soy hydrolysates for identification of productivity markers of mammalian cells for serum-free manufacturing therapeutic proteins

Evolution of feed cell culture media: serum-containing → soy hydrolysate (veggie) → chemically defined

Table 4. Correlation Coefficient (*R*) of Previously Identified Performance Markers When the Soy Hydrolysate Batches were Used for CHO Cell Line #2

LC Method	FA-RP	Amide-HILIC	HFBA(0.1%)-RP
Ion Source	ESI+*	ESI-	ESI+*
Correlation Coefficient			
Negative markers			
Arginine**	-0.71	-0.53	-0.60
Adenosine	-0.44		-0.47
FF	-0.38	-0.36	-0.41
FL	-0.37		-0.38
LF	-0.37		-0.32
LL	-0.45	-0.42	-0.42
FM	-0.42		
LLM	-0.39		
LVF	-0.31		
LLL	-0.39		
VLM	-0.16		
Positive markers (peak area in log scale)			
Phenylalanine	0.10	-0.03	0.28
Valine	0.20		0.24
Isoleucine	0.24		0.25
Lactic acid	0.21		0.28
Succinic acid		0.33	0.47
Citrulline			0.81
Ornithine			0.92

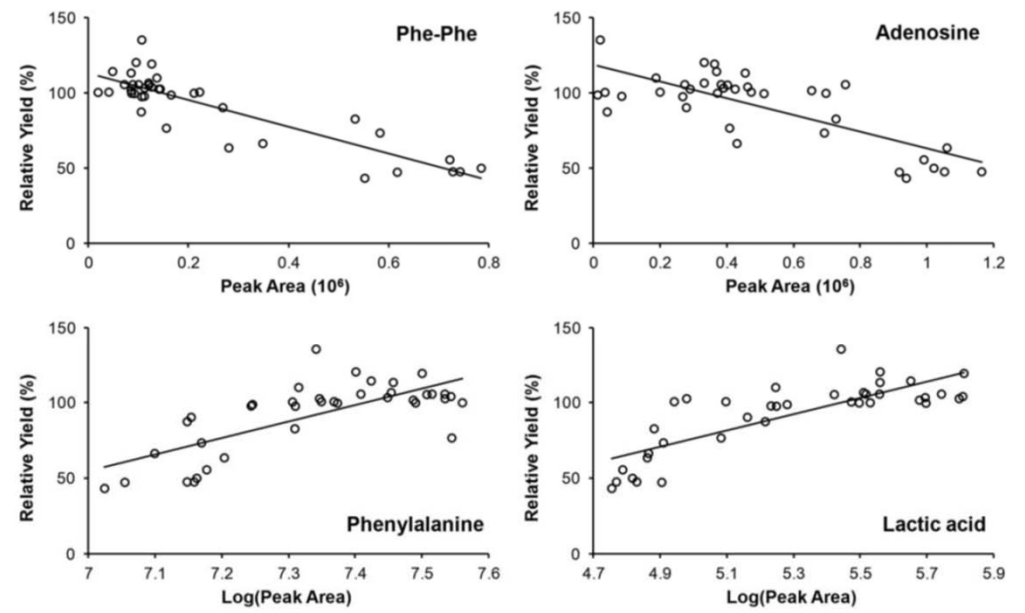


Figure 1. Correlation of a few components with mAb#1 titer (represented as a relative yield). Data obtained using the TDHFA-RP/ESI+ method.

LC-MS/MS metabolomics studies of 30 different soy hydrolysate lots and correlation of metabolite abundances to yield revealed negative (Arginine, adenosine, FF, etc.) and positive (F, V, lactic acid, ornithine, etc.) markers (nutrients) of soy hydrolysates

(Richardson et al., 2015)



Metabolomics analysis of soy hydrolysates for identification of productivity markers of mammalian cells for serum-free manufacturing therapeutic proteins

Table 5. Average Correlation Coefficients of Peptides of Different Lengths with mAb#1 and mAb#2 Titers

Cell Line	#1				#2	
Method	Atlantis-HILIC	ZIC-HILIC	TDFHA-RP	HFBA(0.2%)-RP	FA-RP	HFBA(0.1%)-RP
# of Batches	38	27	38	40	12	12
Peptide Length	Correlation Coefficient				Correlation Coefficient	
1	0.30	0.26	0.43	0.29	-0.04	0.03
2	0.15	0.07	0.29	-0.04	-0.11	-0.03
3	-0.12	-0.15	0.06	-0.06	-0.20	-0.04
4	-0.15	-0.18	-0.08	-0.02	-0.27	-0.16
≥5	-0.15	-0.19	-0.14	-0.06	-0.25	-0.29

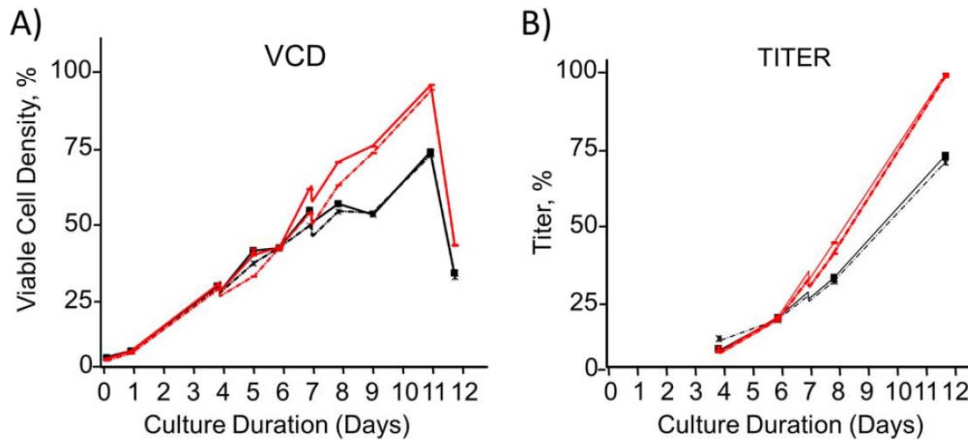


Figure 4. Cell line #2 viable cell density (VCD, A) and productivity (TITER, B) increased after adding 0.1 g/L (760 μM) ornithine to the production medium at the beginning of the 2-liter bioreactor cell culture (in duplicates). Control cell culture runs are shown in black and runs with ornithine addition are shown in red. Both VCD and titer are in relative scale.

- Better soy hydrolysate performance resulted from better bacterial fermentation during the hydrolysate production to individual amino acids and dipeptides.

- When ornithine was spiked into the culture media, both cell lines demonstrated accelerated cell growth, indicating ornithine as a root cause of the performance difference.

(Richardson et al., 2015)

Metabolic markers associated with high mannose (HM) glycan levels of mAbs

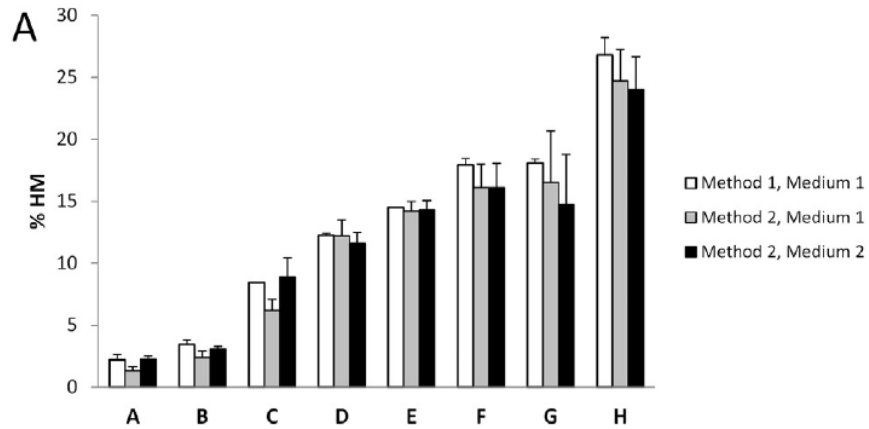


Table 3

Metabolites correlating with high mannose levels obtained from eight-cell line comparison.

Metabolites correlating to HM	Correlation coefficient (media #1)	Correlation coefficient (media #2)
Cystine	0.907	0.877
4-Hydroxybutanoic acid lactone	0.916	0.826
Ornithine	0.803	0.709
Niacinamide	0.881	0.676
Glutathione disulfide	-0.870	-0.846
Glutathione	-0.838	-0.760

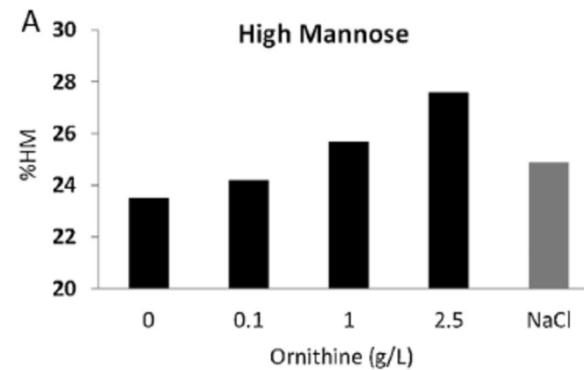
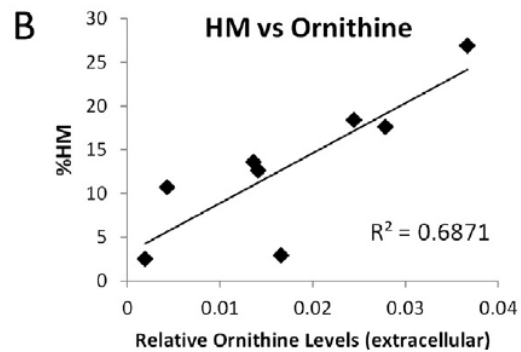


Fig. 5. Correlation between ornithine and high mannose levels from eight-cell line

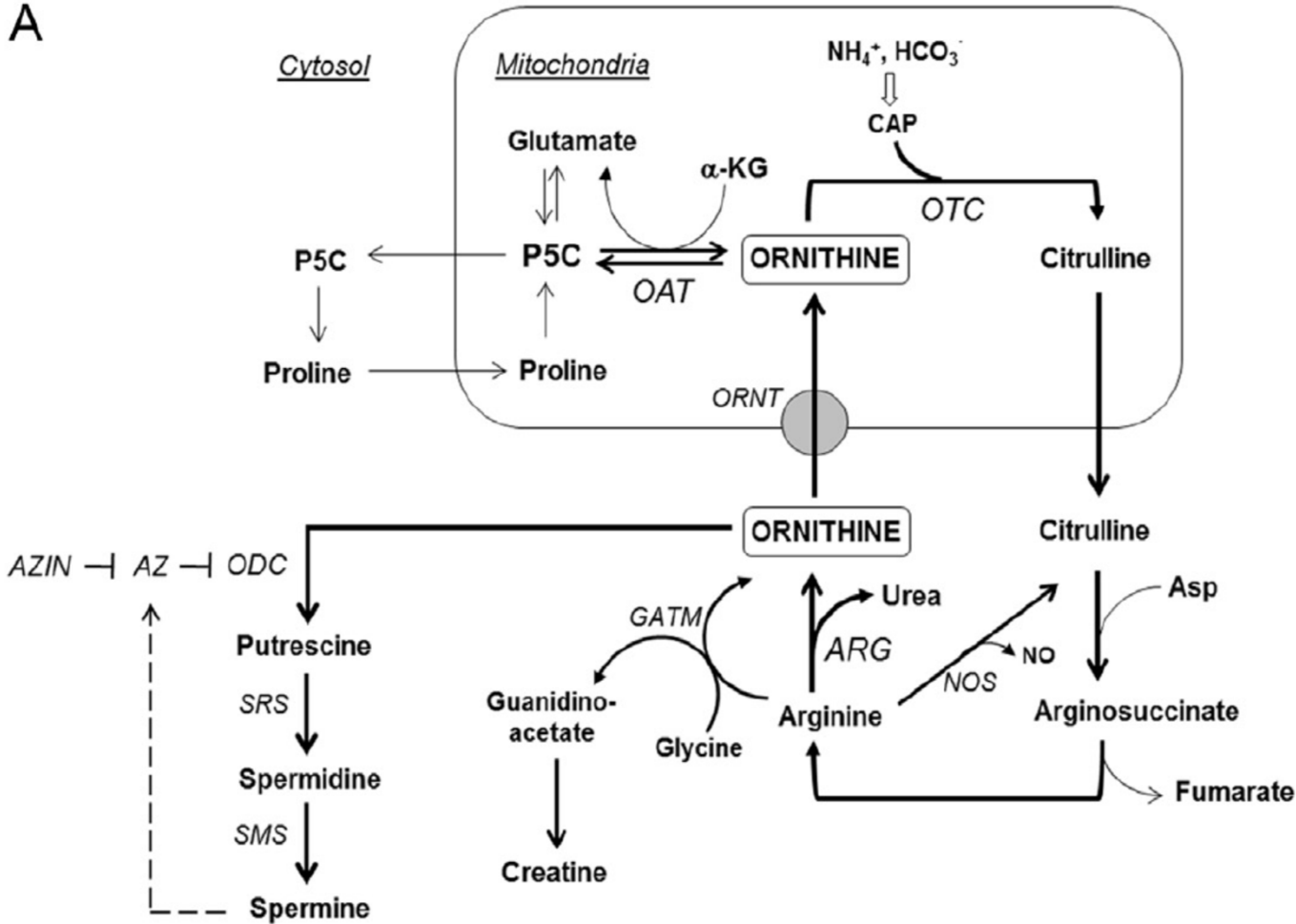
LC-MS/MS metabolomics studies of cell culture media of different cell lines and correlation of metabolite abundances to high mannose revealed several metabolic markers of high mannose including ornithine

Kang et al., 2015



Metabolic markers associated with high mannose glycan (HM) levels of mAbs

A

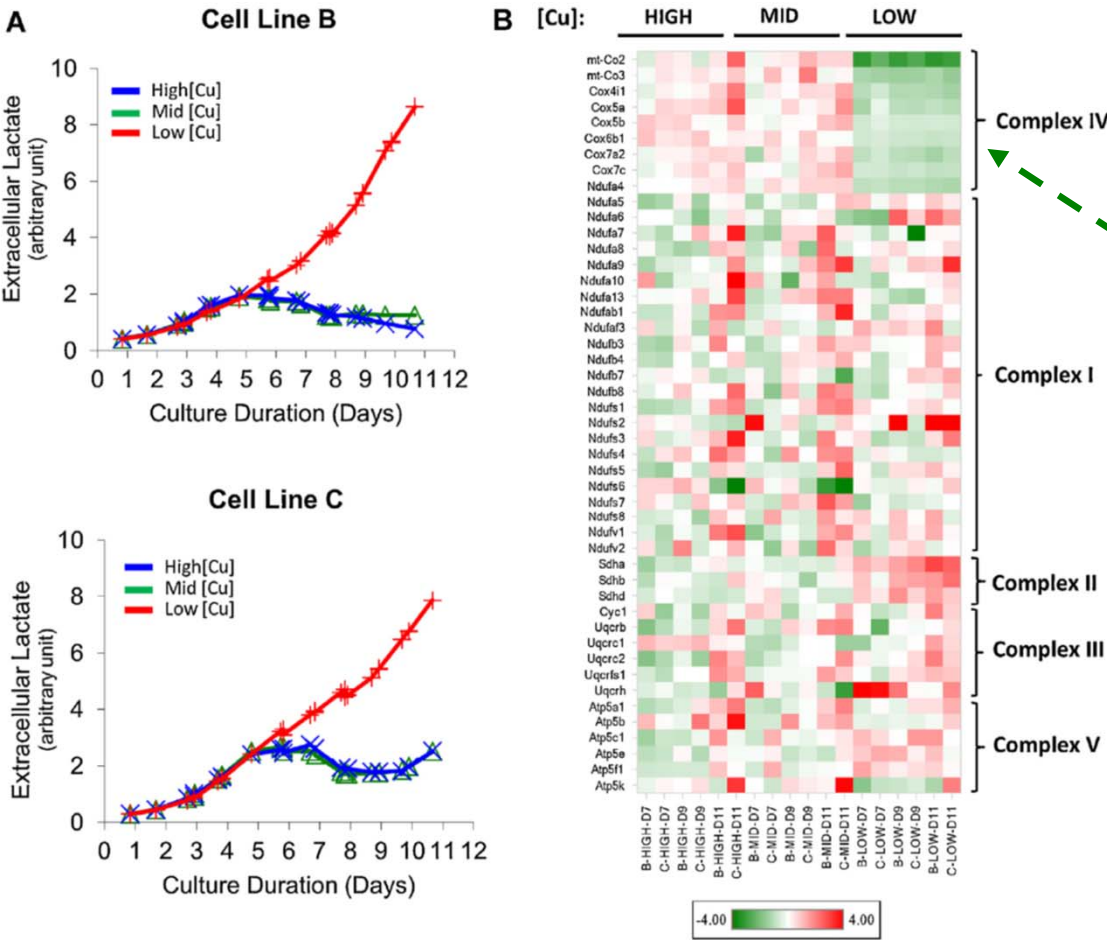


- A strong correlation was also observed between HM and mRNA expression levels of arginase 1 (ARG), an enzyme that catalyzes the conversion of arginine to ornithine.

- Supplementation of ornithine to the culture medium leads to an increased level of HM.

- Reduced concentration of spermine, a downstream product of ornithine metabolism, leads to a decreased level of HM

Proteomics analysis of altered cellular metabolism induced by insufficient copper level

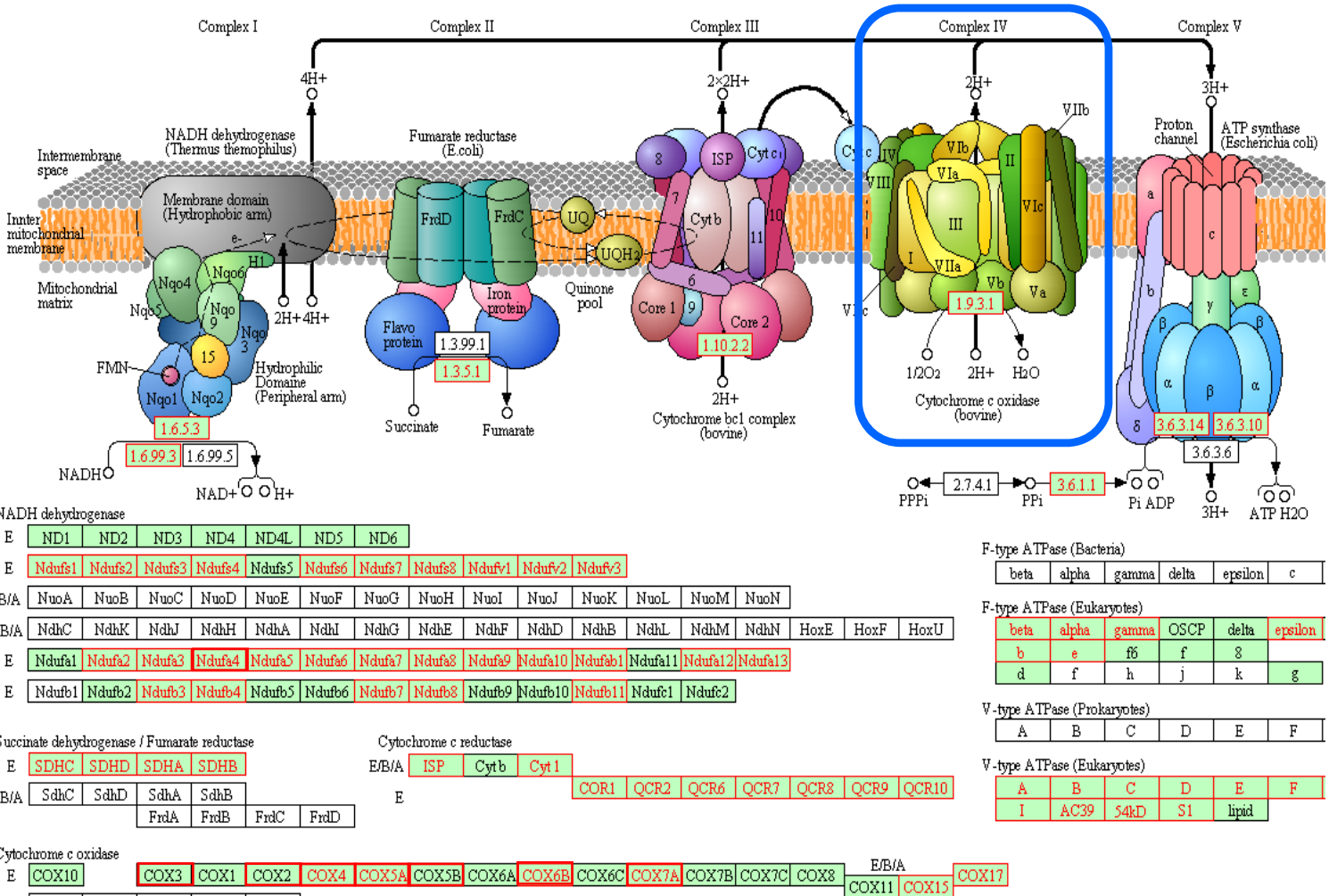


- Method: label-free, LC-MS/MS-based shotgun proteomics
- Results: under copper deficient condition, a substantial reduction of the protein levels of the multiple subunits of Complex IV, also known as cytochrome c oxidase, of the mitochondrial electron transport chain was observed for all three different CHO cell lines expressing therapeutic mAbs

Fig. 5. Copper deficiency-induced lactate accumulation is accompanied by decrease in the protein expression levels of mitochondrial ETC Complex IV proteins in cell lines B and C. (A) Extracellular lactate profiles, (B) Heatmap of ETC complex subunit protein levels. The data represent the relative protein expression profiles obtained from the mouse sequence database search. For cell line B and C, only one of the replicates was analyzed for proteomics analysis.

Kang et al., 2014

Proteomics analysis of altered cellular metabolism induced by insufficient copper level

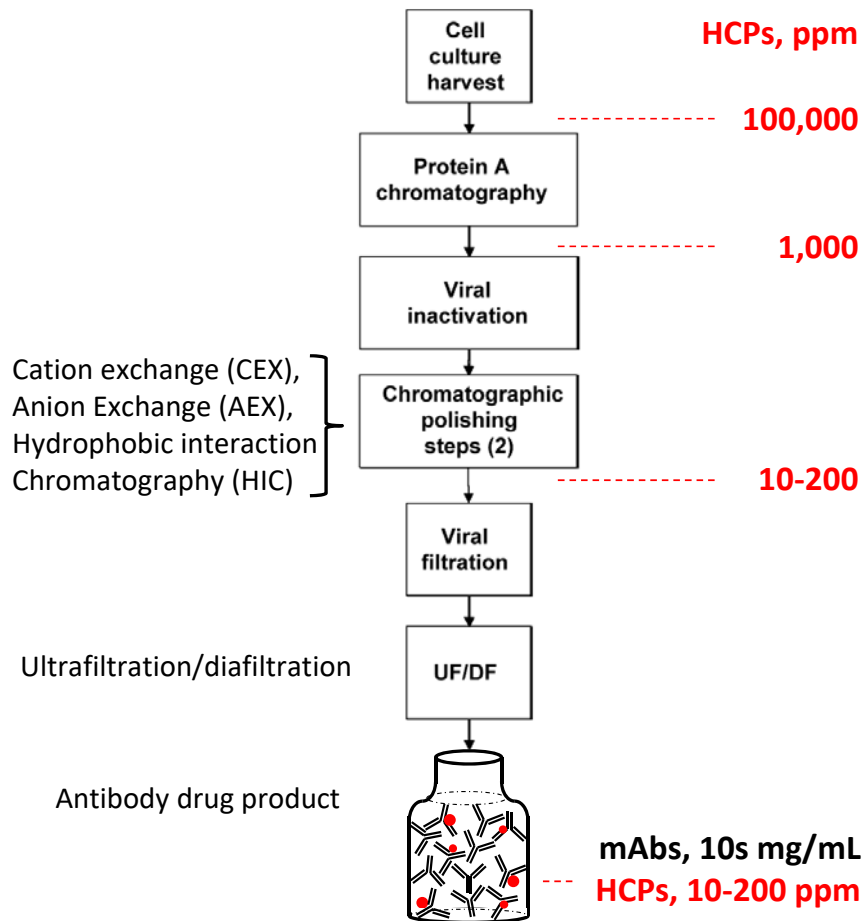


- Label-free, LC-MS/MS-based shotgun proteomics identified majority of proteins from the oxidative phosphorylation pathway in mitochondria (In red)
- Under copper deficient condition, a substantial reduction of the protein levels of the multiple subunits of Complex IV, also known as cytochrome c oxidase (COX), was observed for all three different CHO cell lines expressing therapeutic mAbs
- mRNA levels of COX proteins with normal and low copper were similar. Copper is needed for proper folding of COX proteins.

Kang et al., 2014



Host cell proteins (HCPs) monitoring by LC-MS/MS in therapeutic mAbs

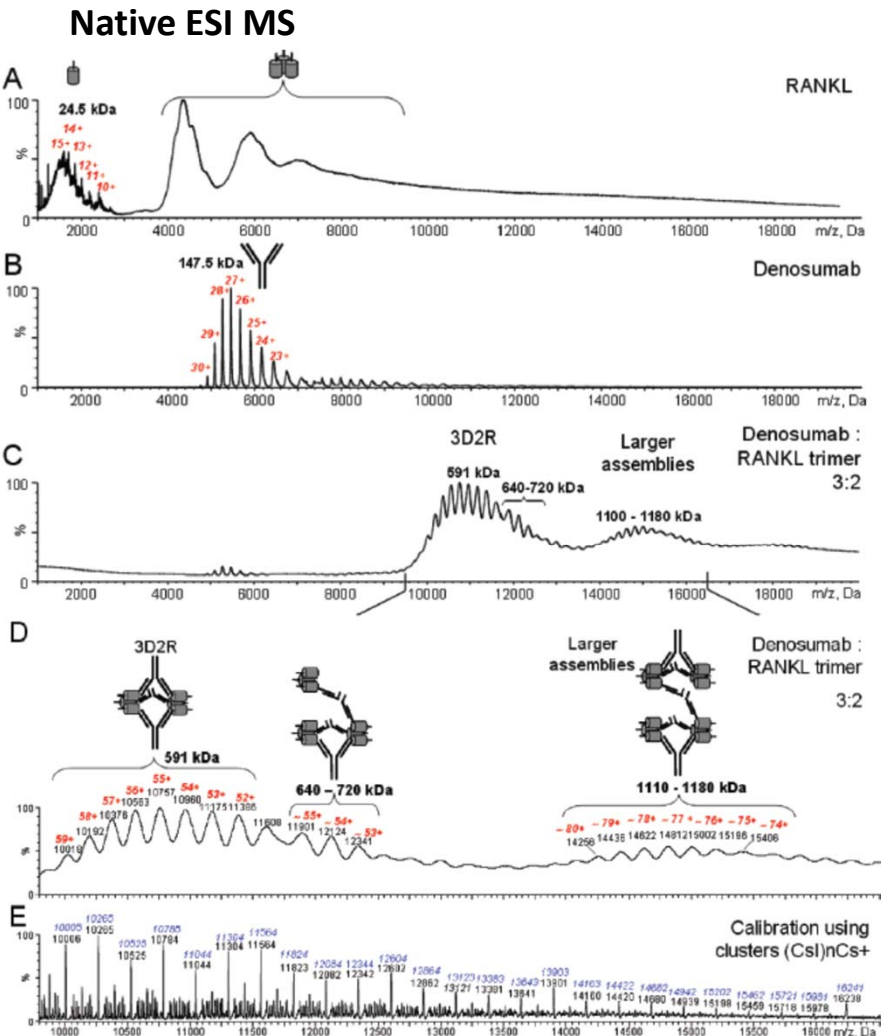


- Soft, non-denaturing purification techniques are used to preserve folding of mAbs.
- Some HCPs remain attached and carried into antibody drug product.
- LC-MS/MS proteomics approach is utilized to identify and quantify host cell proteins in the presence of large concentration of therapeutic protein

Adopted from Shukla, A. A., Hubbard, B., Tressel, T., Guhan, S., and Low, D. (2007), J. Chromatogr. B with modifications

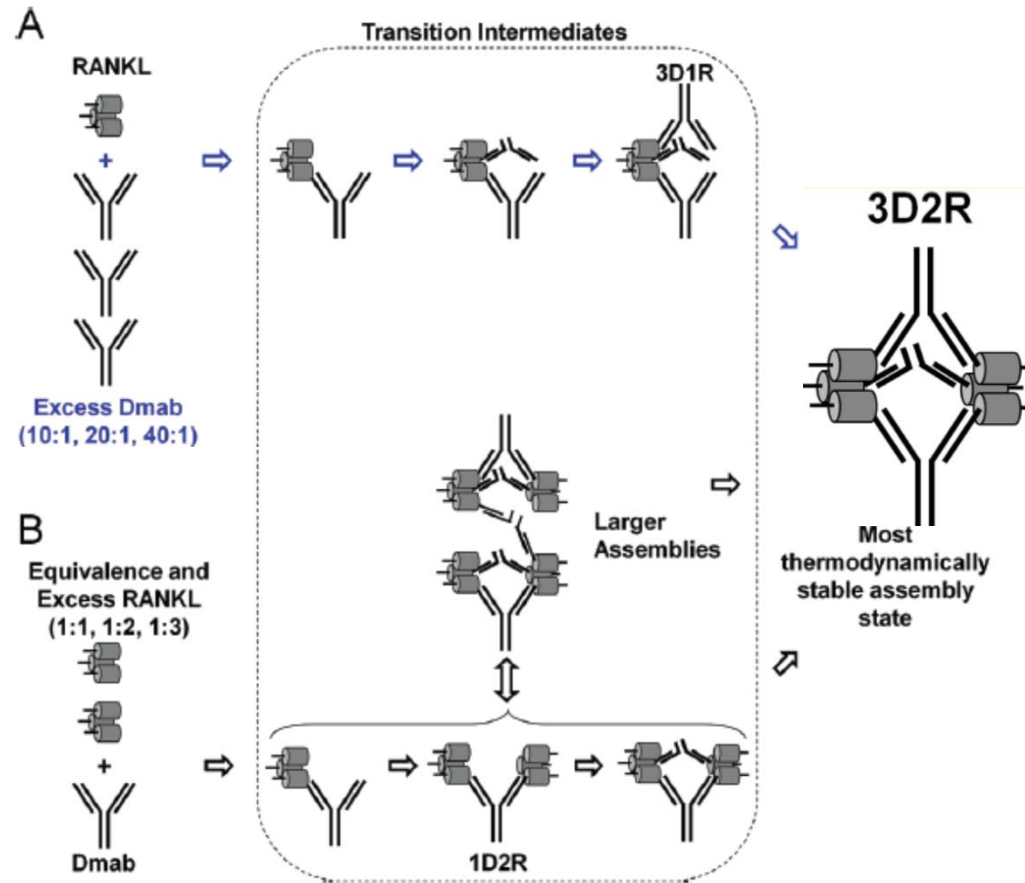


Example of native MS of antibody – antigen interactions



Arthur et al., 2012

Schemes of antibody-antigen complex formation



Stoichiometry of antibody-antigen interactions facilitates elucidation of the mechanism of action

Structural and functional characterization of disulfide isoforms of human IgG2 subclass

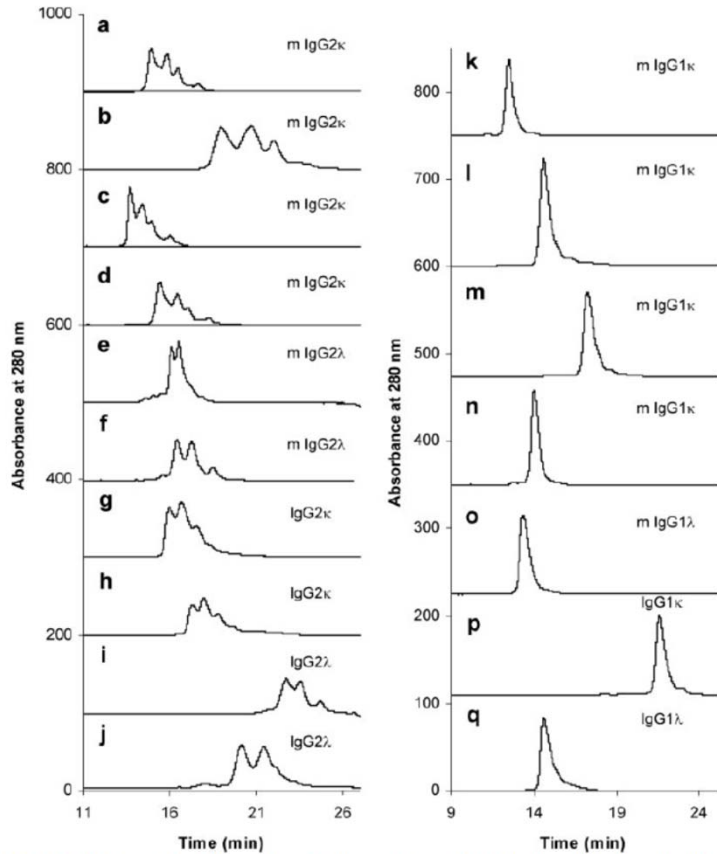


FIGURE 1. RP-HPLC analysis of the two IgG subclasses (IgG1 and IgG2) displayed significantly different profiles by this method. IgG2 antibodies consistently showed heterogeneous profiles with multiple peaks,

Reversed-phase HPLC revealed heterogeneous profiles with multiple peaks for IgG2 and single peak for IgG1 molecules.

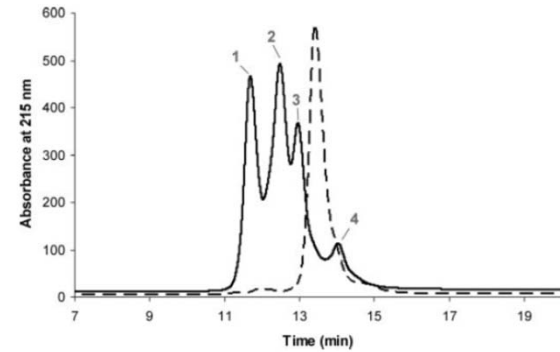


FIGURE 2. RP-HPLC analysis of a human recombinant mAb expressed as an IgG1 (broken line) and IgG2.

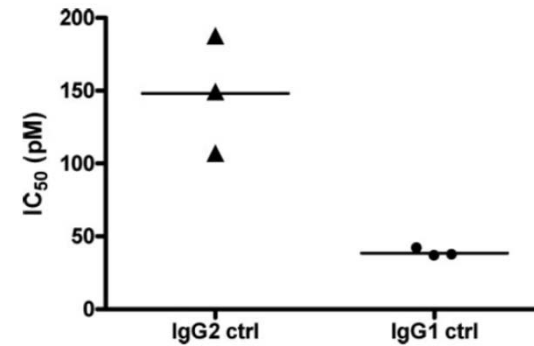
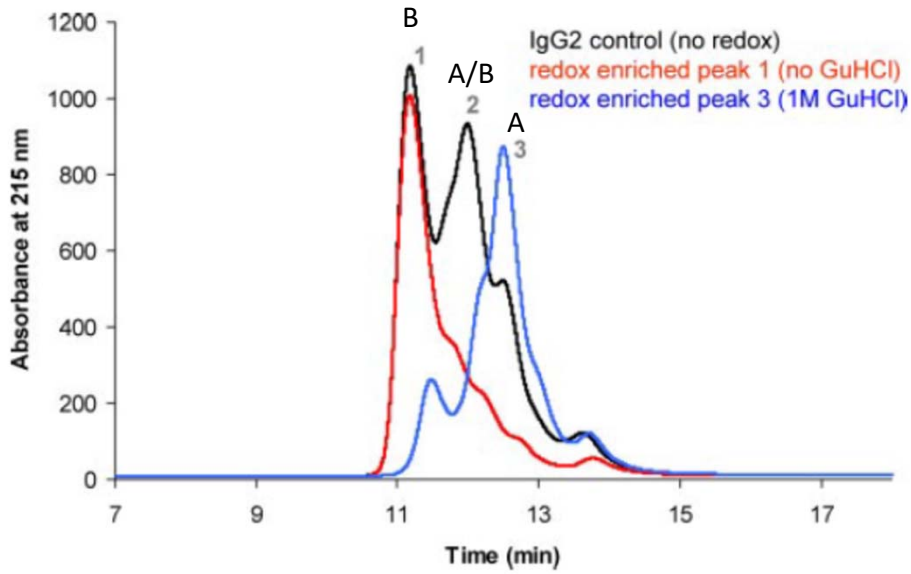


FIGURE 3. IC_{50} values for the inhibition of IL-1 β -induced IL-6 in a chondrocytes assay for the IgG2 (\blacktriangle) and IgG1 (\bullet) mAb constructs are shown ($n = 3$). The black bars represent the means. For statistical analysis the p value was <0.01 .

IgG1 exhibited higher potency as compared to IgG2 in cell based potency assay.

Dillon et al., 2008

Structural and functional characterization of disulfide isoforms of human IgG2 subclass



Redox treatment caused enrichment of different IgG2 disulfide isoforms depending on presence of guanidine

Dillon et al., 2008

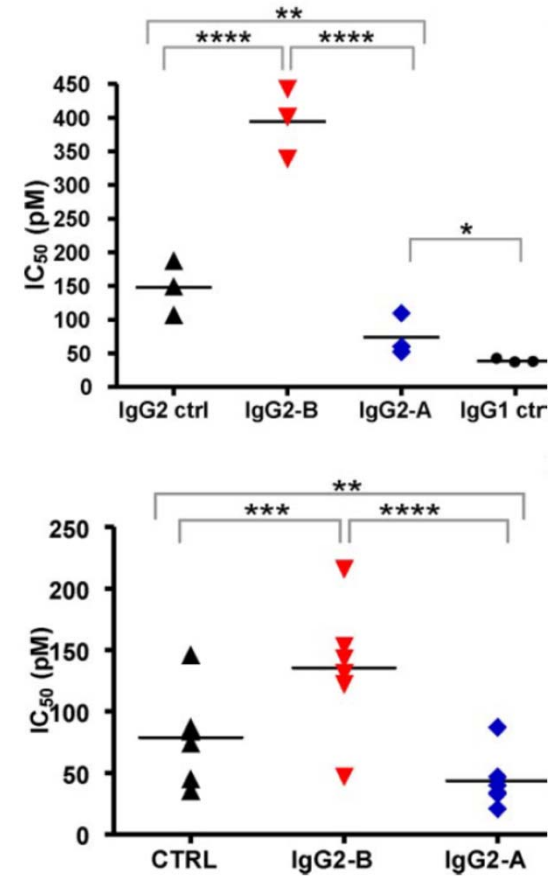


FIGURE 8. Enriched IgG2-A and IgG2-B have different potency. *a, r6*

Enriched IgG2-A disulfide isoform had greater potency as compared to IgG2-B due to greater flexibility and reach of

Structural and functional characterization of disulfide isoforms of human IgG2 subclass

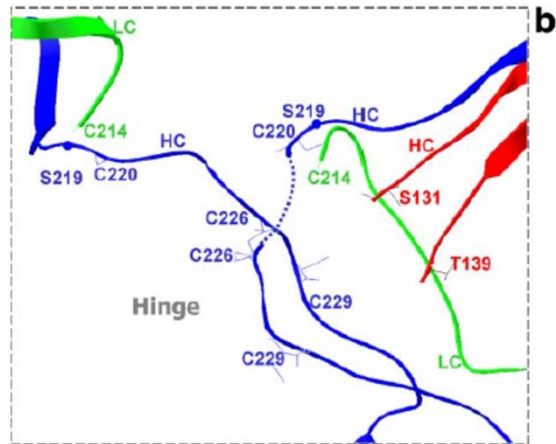
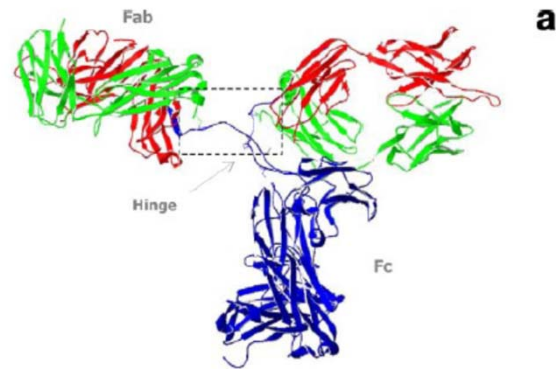
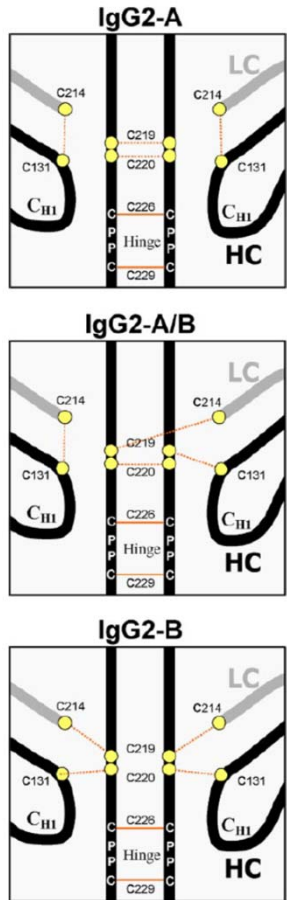
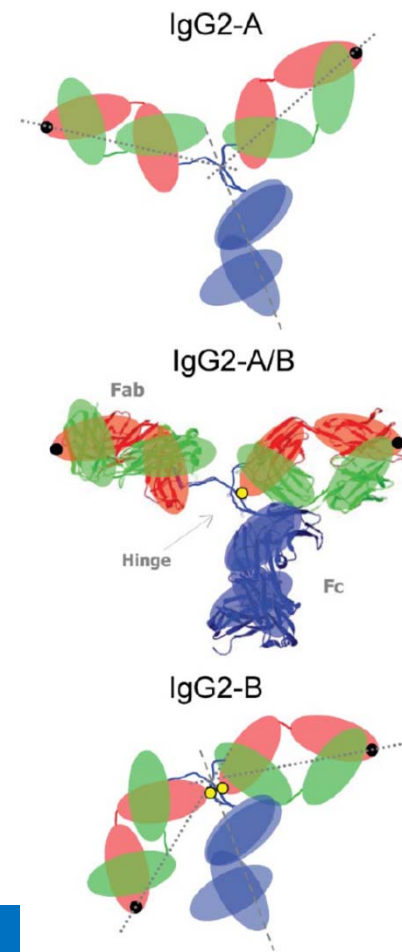


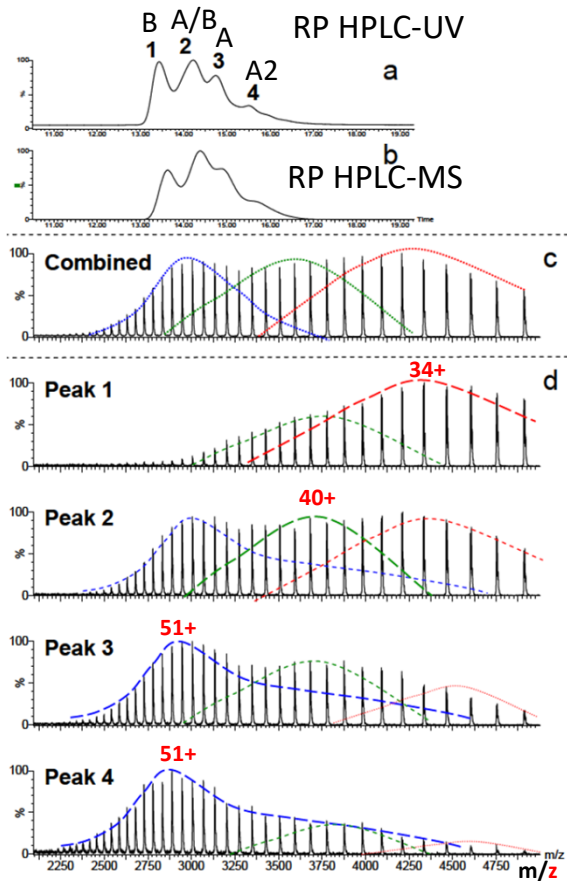
FIGURE 9. A ribbon diagram of a human IgG1 antibody using atomic coordinates that were deposited in the Protein Data Bank (1HZH). The crystal



Dillon et al., 2008; Wypych et al., 2008

- Non-reduced Lys-C peptide mapping uncovered disulfide connectivity of IgG2 disulfide isoforms
- IgG2 disulfide exchange is caused by the close proximity of several cysteine residues at the hinge and the reactivity of tandem cysteines within the hinge

Structural and functional characterization of disulfide isoforms of human IgG2 subclass



ESI mass spectra

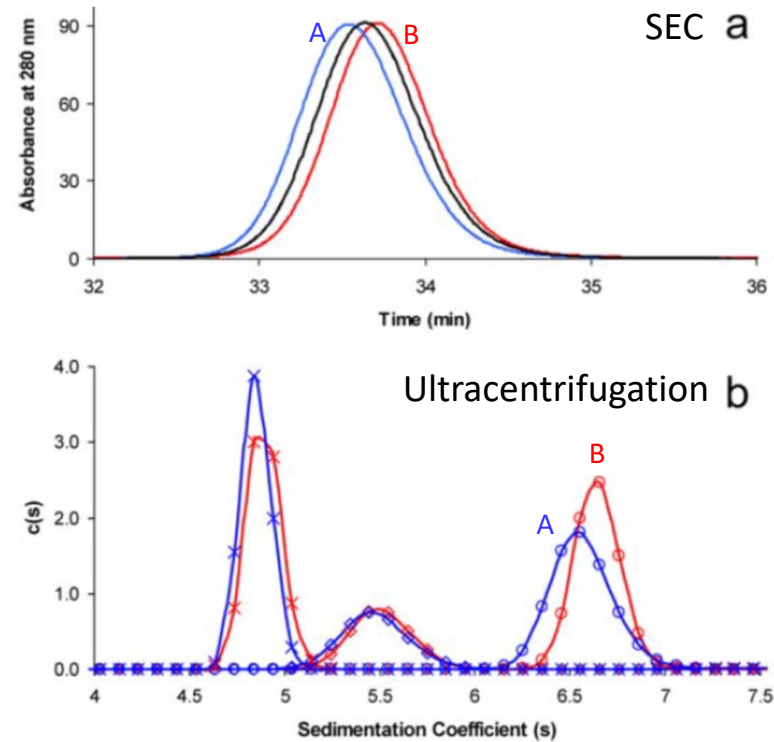


FIGURE 6. Size-exclusion chromatography and sedimentation velocity analysis of the IgG2 redox-enriched samples. *a*, size-exclusion chromatograms of IgG2 control material (black), IgG2-B (red), and IgG2-A (blue) sam-

Size exclusion chromatography and sedimentation velocity analysis revealed larger size (hydrodynamic radius) of native IgG2-A

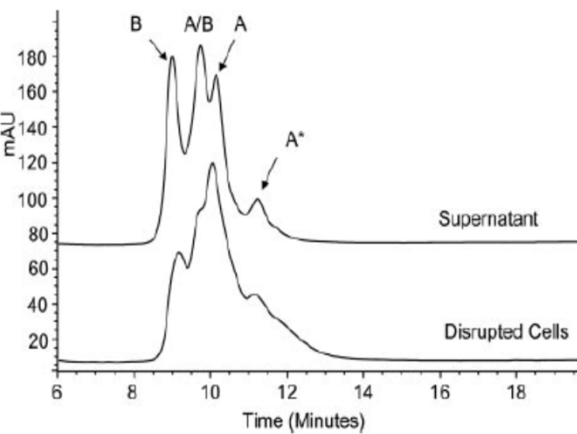
Dillon et al., 2008

IgG2-A isoform (peak 3) eluted later from reversed-phase HPLC and exhibited larger number of charges (lower m/z values) on ESI mass spectra indicating larger size



Biotransformation example: Human IgG2 antibody disulfide rearrangement *in vivo*

In bioreactor



In human blood

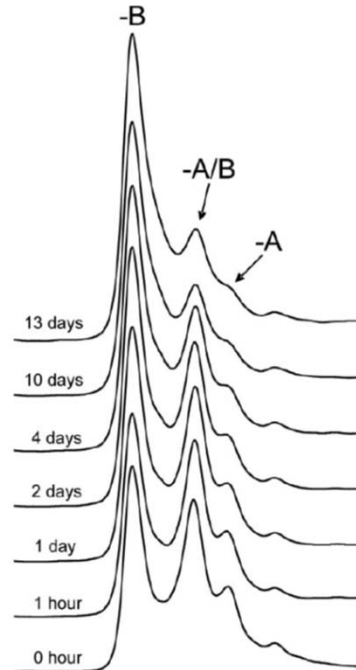


FIGURE 5. RP-HPLC analysis of mAb disulfide variants over time in a single patient. Peaks are labeled as in Fig. 2. Each chromatogram is labeled with the time between dosing and blood withdrawal from this patient.

In human blood

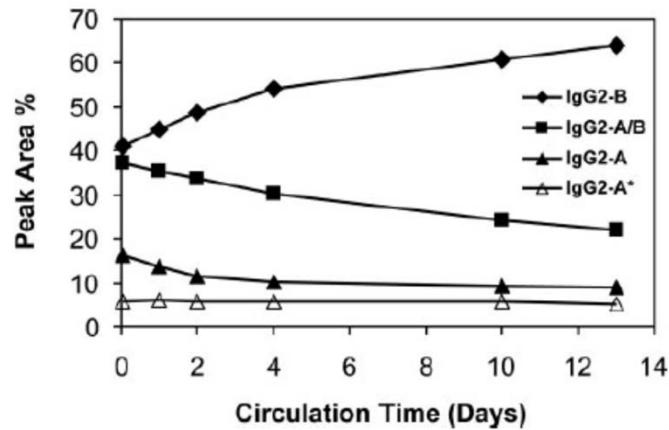
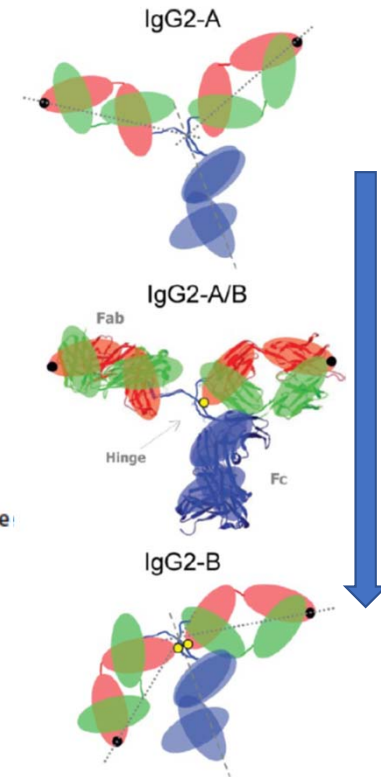


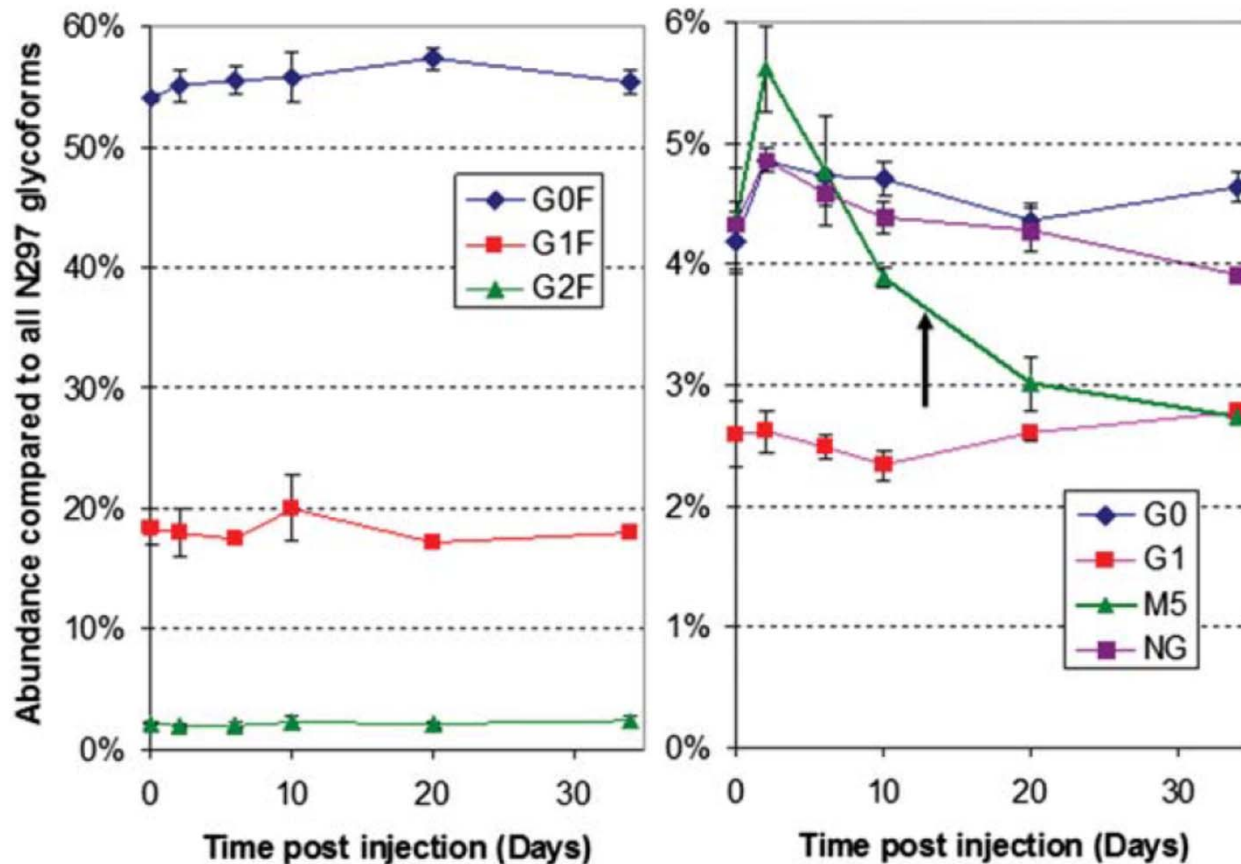
FIGURE 6. Plot of disulfide variant levels versus circulation time in a single patient.



Liu et al., 2008

- IgG2 disulfide linkages interconvert while circulating in humans.
- Secretory cells initially produce primarily one form (IgG2-A), which is rapidly converted to a second form (IgG2-A/B) while circulating in blood, followed by a slower conversion to a third form (IgG2-B).
- In case of the recombinant therapeutic IgG2 antibodies, similar IgG2-A → IgG2-A/B → IgG2-B conversion first takes place in redox environment of bioreactor and then continues in human blood after administration

PK example: High-mannose 5 glycans (M5) on Fc of therapeutic IgG antibodies increase serum clearance in humans



- The therapeutic IgGs were affinity purified from serum samples from human PK studies, and changes to the glycan profile over time were determined by peptide mapping.
- Relative levels of high-mannose 5 (M5) glycan decreased as a function of circulation time, whereas other glycans remained constant.
- These results demonstrate that therapeutic IgGs containing Fc high-mannose glycans are cleared more rapidly in humans than other glycan forms.

Goetze et al., 2011

PK example: High-mannose 5 glycans (M5) on Fc of therapeutic IgG antibodies increase serum clearance in humans

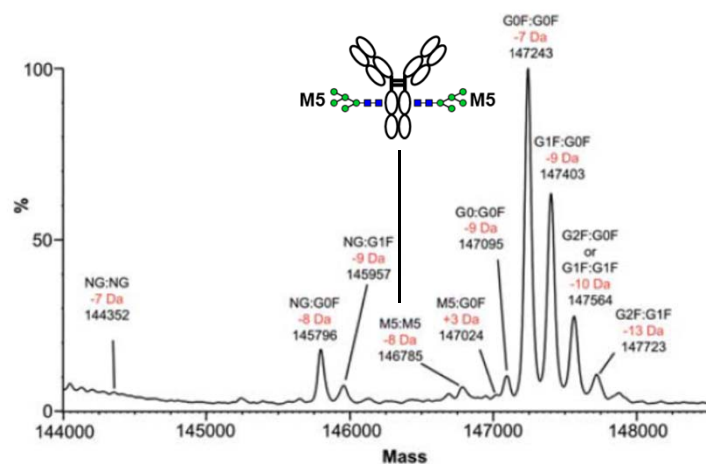


Fig. 2. Deconvoluted ESI mass spectrum of Mab1. y-axis represents the ion intensity. Each peak is labeled (top to bottom) with composition of major oligosaccharide pairs, experimental deviation from theoretical mass and measured mass. The elevated baseline at mass <144,500 is due to a MaxEnt 1 deconvolution artifact. NG, non-glycosylated.

Table V. Summary results for the calculation of percent of each Mab containing at least one Fc M5 glycan

	Mab1	Mab2	Mab3	Mab4
M5 by peptide map (%)	5.0	12.2	4.0	17.0
M5:M5 PP	~50	8.8	6.4	8.8
Calculated % of Mab containing M5 (%)	5.1	13.4	4.6	18.6

M5:M5 PP is defined as the experimental (M5:M5)/(M5:G0F) ratio divided by that expected from random pairing of heavy chains (see text for further details).

Mab ligand affinity purifications

Ligand-based affinity purification of Mabs was carried out essentially as described previously. Briefly, a 0.5 mL aliquot of freshly clarified human serum-containing Mab was diluted with 4.5 mL of phosphate-buffered saline (PBS) and incubated with 0.2 mL of Mab-ligand resin. Soluble forms of the appropriate receptor were used as the ligand when the Mab target

- There is a strong, but not exclusive, preference for M5:M5 pairing, the degree of which may vary among molecules.
- In this study, however, the impact of M5 on antibody clearance is not significantly greater than that calculated based on M5 fraction per heavy chain.

Goetze et al., 2011

References and acknowledgements

- Bailey AO, Han G, Phung W, Gazis P, Sutton J, Josephs JL, Sandoval W. 2018.** Charge variant native mass spectrometry benefits mass precision and dynamic range of monoclonal antibody intact mass analysis. *mAbs* **10**: 1214-1225.
- Bondarenko PV, Second TP, Zabrouskov V, Makarov AA, Zhang Z. 2009.** Mass measurement and top-down HPLC/MS analysis of intact monoclonal antibodies on a hybrid linear quadrupole ion trap-Orbitrap mass spectrometer. *J.Am.Soc.Mass Spectrom.* **20**: 1415-1424.
- Bondarenko PV, Xiao G, Dillon TM, Zhang Z. 2010.** Localization and quantification of free sulfhydryl in monoclonal antibodies by top-down HPLC/MS analysis. *Proc 58th ASMS Conf Mass Spectrom Allied Topics, Salt Lake City, Utah, May 23-27, 2010.*
- Arthur KK, Gabrielson JP, Hawkins N, Anafi D, Wypych J, Nagi A, Sullivan JK, Bondarenko PV., 2012** In vitro stoichiometry of complexes between the soluble RANK ligand and the monoclonal antibody denosumab. *Biochemistry*, **51**, 795–806
- Chelius D, Xiao G, Nichols AC, Vizel A, He B, Dillon TM, Rehder DS, Pipes GD, Kraft E, Oroska A, Treuheit MJ, Bondarenko PV. 2008.** Automated tryptic digestion procedure for HPLC/MS/MS peptide mapping of immunoglobulin gamma antibodies in pharmaceuticals. *J.Pharm.Biomed.Anal.* **47**: 285-294.
- Chu GC, Chelius D, Xiao G, Khor HK, Coulibaly S, Bondarenko PV. 2007.** Accumulation of succinimide in a recombinant monoclonal antibody in mildly acidic buffers under elevated temperatures. *Pharm.Res.* **24**: 1145-1156.
- Dillon TM, Bondarenko PV, Rehder DS, Pipes GD, Kleemann GR, Ricci MS. 2006.** Optimization of a reversed-phase LC/MS method for characterizing recombinant antibody heterogeneity and stability. *J.Chromatogr.A* **1120**: 112-120.
- Dillon TM, Speed-Ricci M, Vezina C, Flynn GC, Liu YD, Rehder DS, Plant M, Henkle B, Li Y, Varnum B, Wypych J, Balland A, Bondarenko PV. 2008.** Structural and functional characterization of disulfide isoforms of the human IgG2 subclass. *J.Biol.Chem.* **283**: 16206-16215.
- Goetze AM, Liu YD, Zhang Z, Shah B, Lee E, Bondarenko PV, Flynn GC. 2011.** High-mannose glycans on the Fc region of therapeutic IgG antibodies increase serum clearance in humans. *Glycobiology* **21**: 949-959.
- Harris RJ, Kabakoff B, Macchi FD, Shen FJ, Kwong MY, Andya JD, Shire SJ, Bjork N, Totpal K, Chen AB. 2001.** Identification of multiple sources of charge heterogeneity in a recombinant antibody. *J.Chromatogr.B Biomed.Sci.Appl.* **752**: 233-245.

References and acknowledgements

Hartl FU, Hayer-Hartl M. 2009. Converging concepts of protein folding in vitro and in vivo. *Nat Struct.Mol.Biol.* **16:** 574-581

Kang S, Xiao G, Ren D, Zhang Z, Le N, Trentalange M, Gupta S, Lin H, Bondarenko PV. 2014. Proteomics analysis of altered cellular metabolism induced by insufficient copper level. *J.Biotechnol.* **189:** 15-26.

Kang S, Zhang Z, Richardson J, Shah B, Gupta S, Huang CJ, Qiu J, Le N, Lin H, Bondarenko PV. 2015. Metabolic markers associated with high mannose glycan levels of therapeutic recombinant monoclonal antibodies. *J Biotechnol* **203:** 22-31.

Kleemann GR, Beierle J, Nichols AC, Dillon TM, Pipes GD, Bondarenko PV. 2008. Characterization of IgG1 immunoglobulins and peptide-Fc fusion proteins by limited proteolysis in conjunction with LC-MS. *Anal. Chem.* **80,** 2001-2009

Lin TJ, Beal KM, Brown PW, DeGruttola HS, Ly M, Wang W, Chu CH, Dufield RL, Casperson GF, Carroll JA, Friese OV, Figueroa B, Jr., Marzilli LA, Anderson K, Rouse JC. 2019. Evolution of a comprehensive, orthogonal approach to sequence variant analysis for biotherapeutics. *mAbs* **11:** 1-12.

Liu YD, Chen X, Enk JZ, Plant M, Dillon TM, Flynn GC. 2008. Human IgG2 antibody disulfide rearrangement in vivo. *J.Biol.Chem.* **283:** 29266-29272.

Masuda K, Yamaguchi Y, Kato K, Takahashi N, Shimada I, Arata Y. 2000. Pairing of oligosaccharides in the Fc region of immunoglobulin G. *FEBS Lett.* **473:** 349-357.

Rehder DS, Chelius D, McAuley A, Dillon TM, Xiao G, Crouse-Zeineddini J, Vardanyan L, Perico N, Mukku V, Brems DN, Matsumura M, Bondarenko PV. 2008. Isomerization of a single aspartyl residue of anti-epidermal growth factor receptor immunoglobulin gamma 2 antibody highlights the role avidity plays in antibody activity. *Biochemistry* **47:** 2518-2530.

Ren D, Pipes GD, Liu D, Shih LY, Nichols AC, Treuheit MJ, Brems DN, Bondarenko PV. 2009. An improved trypsin digestion method minimizes digestion-induced modifications on proteins. *Anal.Biochem.* **392:** 12-21.

Richardson J, Nicklaus M, Shah B, Bondarenko PV, Bhebe P, Kombe MC, Zhang Z. 2015. Metabolomics analysis of soy hydrolysates for the identification of productivity markers of mammalian cells for manufacturing therapeutic proteins. *Biotech.Prog.* **31:** 522-531.

Richardson J, Shah B, Xiao G, Bondarenko PV, Zhang Z. 2011. Automated in-solution protein digestion using a commonly available high-performance liquid chromatography autosampler. *Anal.Biochem.* **411:** 284-291.

References and acknowledgements

Shi L, Xiao G, Dillon TM, Ricci MS, Bondarenko PV. 2019. Cation-exchange chromatography - mass spectrometry and top-down analysis of therapeutic proteins. *67th ASMS Conference on Mass Spectrometry, June 2-6, 2019, Atlanta, Georgia, manuscript is submitted for publication.*

Valliere-Douglass J, Marzilli L, Deora A, Du Z, He L, Kumar S, Liu YH, Martin-Mueller H, Nwosu C, Stults J, Wang Y, Yaghmour S, Zhou Y. 2019. Biopharmaceutical Industry Practices for Sequence Variant Analyses of Recombinant Protein Therapeutics. *PDA.J Pharm.Sci.Technol.*

Wong HE, Huang CJ, Zhang Z. 2018. Amino acid misincorporation in recombinant proteins. *Biotechnol Adv.* **36**: 168-181.

Wypych J, Li M, Guo A, Zhang Z, Martinez T, Allen M, Fodor S, Kelner D, Flynn GC, Liu YD, Bondarenko PV, Speed-Ricci M, Dillon TM, Balland A. 2008. Human IgG2 antibodies display disulfide mediated structural isoforms. *J.Biol.Chem.* **283**: 16194-16205.

Xiao G, Ren D, Bondarenko PV. 2014. Size-based enrichment and 1D LC-MS/MS analysis of low ppm levels of host cell proteins in high-concentration antibody drugs. *Proceedings 62nd ASMS Conference, Baltimore, MD.*

Zhang Z, 2011 Prediction of collision-induced-dissociation spectra of peptides with post-translational or process-induced modifications. *Anal. Chem.* **83**, 8642–8651

Thank you CASSS MASS SPEC 2019!
Thank you Chicago!

